Chapter SM (Structural Modeling)

A BALANCED CROSS SECTION AND KINEMATIC AND THERMAL MODEL ACROSS THE NORTHEASTERN BROOKS RANGE MOUNTAIN FRONT, ARCTIC NATIONAL WILDLIFE REFUGE, ALASKA

by F. Cole[1], K.J. Bird[1], C.G. Mull[2], W.K. Wallace[3], W. Sassi[4], J.M. Murphy[5], and M. Lee[6]

in The Oil and Gas Resource Potential of the 1002 Area, Arctic National Wildlife Refuge, Alaska, by ANWR Assessment Team, U.S. Geological Survey Open-File Report 98-34.

1999

[1] U.S. Geological Survey, Menlo Park, California
[2] State of Alaska Division of Geological and Geophysical Surveys, Fairbanks, Alaska
[3] University of Alaska, Fairbanks, Alaska
[4] Institut Français du Pétrole, Paris, France
[5] University of Wyoming, Laramie, Wyoming
[6] U.S. Geological Survey, Denver, Colorado

TABLE OF CONTENTS

FIGURES

Click here or on this symbol in the toolbar to return.

PLATE

TABLE

Click here or on this symbol in the toolbar to return.

ABSTRACT

We constructed a balanced cross section and structural-stratigraphic restoration of a transect in the northeastern Brooks Range, Alaska, in the northern part of the Arctic National Wildlife Refuge. The transect extends from the coastline southward to the Fourth Range and crosses the transition between the foreland basin and the frontal part of the Brooks Range thrust belt. We developed a kinematic and thermal model to examine the main stages of deformation, sedimentation, and oil source rock maturation associated with the Brookian orogeny in this area. Timing of events in the model was constrained by fission-track ages from the thrust belt and ages of stratigraphic units that are preserved in the foreland basin.

The model begins with southward flexure and foreland basin sedimentation in Early Cretaceous to Early Eocene time, presumably caused by crustal thickening south of the transect area during early stages of Brookian orogeny. This is followed by uplift and erosion of the southern part of the transect in the Middle Eocene, as orogenesis advanced northward and the area from the Fourth Range to the Sadlerochit Mountains became involved in a basement-cutting duplex system. Sedimentation in the foreland continued after Middle Eocene deformation, but the basin depocenter shifted north of the Sadlerochit Mountains. Continued northward propagation of the basement duplex system in Middle to Late Oligocene time produced a second stage of uplift and erosion from the Fourth Range to the Sadlerochit Mountains and initial growth of the Marsh Creek anticline. Finally, out-of-sequence faulting accompanied by uplift and erosion in Neogene to Recent time resulted in the topographic relief that we see today at the Shublik and Sadlerochit Mountain fronts.

According to the sequential stages of burial, uplift, and erosion prescribed by this model, the thermal history of rocks in the southern part of the transect began with progressive heating in Early Cretaceous to Early Eocene time, followed by episodic cooling in the Middle Eocene and Oligocene, and possibly a third cooling episode in Miocene to Recent time. The thermal history for the rocks in the northern part of the transect, i.e., north of the Marsh Creek anticline, is characterized by progressive heating from Early Cretaceous to Recent time.

Oil-prone source rocks in the Shublik Formation attained thermal maturity and began to generate oil in Late Cretaceous to Paleocene time, before the

growth of the Brookian structures on this transect. Regional southward flexure of the transect area at that time favored migration toward the north, i.e., toward the distal part of the foreland. A small wedge of the Shublik Formation near its northern limit may have generated oil later, after the onset of deformation in the Shublik and Sadlerochit Mountains. This oil may have migrated southward into the Shublik-Sadlerochit structural high-- a feature now breached by erosion. Stratigraphically higher petroleum source rocks, i.e., in the Hue Shale and Canning Formation were not modeled in this study, but other studies show that these units generated oil after formation of structural traps associated with the Brookian orogeny.

INTRODUCTION

We undertook this study in order to characterize the history of deformation, sedimentation, and petroleum generation along a transect across the northeastern salient of the Brooks Range, near the northwestern boundary of the Arctic National Wildlife Refuge (Fig. SM1). The study was conducted as part of a larger effort by the U.S. Geological Survey to assess the oil and gas resource potential of the 1002 area-- the northern 8% of the Arctic National Wildlife Refuge that was set aside by Congress in 1980 for petroleum exploration. With this study, we have tried to provide an integrated and objective look at the geologic history and certain aspects of the petroleum potential in the northwestern corner of the wildlife refuge, near the western boundary of the 1002 area. We intend this study to be used along with other scientifically based analyses to aid in decisions about the future land status of the 1002 area. We received supplemental funding and logistical support from Stanford University and the Institut Français du Pétrole.

First we present a balanced geological cross-section of the transect area, and explain the data that went into making the cross-section, including borehole data, seismic stratigraphy, and geologic data observed in outcrops. Then we present a kinematic model that illustrates a possible scenario for the history of sedimentation and deformation along the transect, based on stratigraphic, structural, and thermochronologic constraints. Finally, on the basis of quantitative models computed with the software Thrustpack, we discuss the thermal history prescribed by the kinematic scenario, including the specific maturation history of oil-prone source rocks, and the implications for the timing and favorability of petroleum generation in the transect area.

Thrustpack is a software package developed by the Institut Français du Pétrole for modeling deformation, sedimentation, and kerogen maturation in fold and thrust belts.

BALANCED GEOLOGIC CROSS SECTION

Our transect is located at the juncture between the northeastern salient of the Brooks Range orogen and the North Slope foreland basin (Figs. SM1 and SM2). Both features were produced by the Brookian orogeny, a Jurassic through Tertiary event that affected most of northern Alaska (Mull, 1982; Moore et al., 1994). In the northeastern Brooks Range, most deformation associated with the Brookian orogeny occurred in the Tertiary, while to the west, in the main axis of the Brooks Range, most of the shortening was in Jurassic and Cretaceous time (Moore et al., 1994).

The transect is 100 km in length, starting to the south in the Fourth Range, within the thrust belt, and terminating to the north at Flaxman Island, in the undeformed part of the foreland basin (Fig. SM2, Plate SM1). It traverses the prominent structures at the leading edge of the thrust belt, including the Shublik and Sadlerochit Mountains, and the more subdued Marsh Creek anticline, which is the northernmost contractional structure associated with the Brookian orogeny on this transect.

The southern part of the transect (A-D on Fig. SM2 and Plate SM1) is located in the mountainous region or "outcrop belt," where bedrock exposures are very good and the regional geology is well-known. Our interpretation in the outcrop belt is based largely on the regional Canning River section of Wallace and Hanks (1990) and Wallace (1993), located about 7 km to the east of our transect. Other structural interpretations in the same general area include Leiggi (1987), Rattey (1987), Kelley and Foland (1987), and Kelley and Molenaar (1987).

The northern part of the transect (E-G on Fig. SM1) follows the location of seismic lines AN84-6 (E-F) and AN85-8 (F-G), which provide the basis for our interpretation across this largely tundra-covered, coastal plain region. These seismic lines were published previously in U.S. Geological Survey Bulletin 1778 (Bird and Magoon, 1987). Reports from several exploratory wells near Flaxman Island (Location G), and from shot-hole paleontologic samples collected along seismic line AN84-6 (near location E), provide valuable stratigraphic and biostratigraphic control for the interpretation of

the foreland basin stratigraphy beneath the coastal plain. We also based our interpretation of the foreland basin stratigraphy on the reports of Bird (Chap. GG) and Houseknecht and Schenk (Chap. BS).

STRATIGRAPHY

Three main stratigraphic sequences are present in the northeastern Brooks Range and in the area of our transect: (1) the pre-Mississippian sequence, (2) the Ellesmerian sequence, and (3) the Brookian sequence (Plate SM1a, Fig. SM3; Lerand, 1973; Grantz et al., 1975; Bird and Molenaar, 1987). The boundaries between these sequences correspond approximately with two regional unconformities-- the sub-Mississippian unconformity (SMU), which separates the pre-Mississippian from the overlying Ellesmerian sequence, and the Lower Cretaceous unconformity (LCU), which occurs in the upper part of the Ellesmerian sequence near the base of the Brookian sequence.

The sub-Mississippian unconformity reflects an episode of regional uplift and erosion probably related to late stages of the Ellesmerian orogeny. In the northeastern Brooks Range, evidence for this orogeny comes from brittle and ductile contractional structures in the pre-Mississippian sequence that are beveled flat beneath the unconformity.

The Lower Cretaceous unconformity occurs just below the stratigraphic horizon separating northern-sourced passive margin deposits of the Ellesmerian sequence from southern-sourced orogenic clastic deposits of the Brookian sequence (Fig. SM3). The unconformity is Hauterivian in age, or about 130 Ma, according to the Gradstein et al. (1994) time scale, while the provenance reversal is Barremian (ca. 125 Ma) in this area, based on the age of the boundary between the pebble shale unit and the Hue Shale (Bird and Molenaar, 1987). The Lower Cretaceous unconformity is thought to be the break-up unconformity related to the separation of northern Alaska from the Canadian Arctic islands or some other landmass that formerly occupied the area north of the coast (Grantz and May, 1983).

The pre-Mississippian and Ellesmerian sequences are well-exposed in the mountains, where their stratigraphy is well-known (Bird and Molenaar, 1987; Robinson et al., 1989). The Brookian sequence is present mainly beneath the coastal plain, and its stratigraphy is known from scattered outcrops, from wells along the Canning River and near the coast, and from

seismic stratigraphy beneath the coastal plain (Molenaar et al., 1986; Bird and Molenaar, 1987; Bird, 1998; Houseknecht and Schenk, Chap. BS).

Pre-Mississippian Sequence

The pre-Mississippian sequence includes all of the rocks that underlie the sub-Mississippian unconformity in the transect area. It is often referred to as "basement" in this region, because it is generally more penetratively deformed than the overlying Ellesmerian sequence (Moore et al., 1994). In the Shublik and Sadlerochit Mountains, however, competent units in the upper part of the sequence show remarkably little internal strain, unlike rocks of the pre-Mississippian sequence exposed elsewhere in the northeastern Brooks Range.

The structural geometry within the pre-Mississippian sequence is characterized by large-scale fault-bend folding that produces anticlinal uplifts in the Sadlerochit and Shublik Mountains and the area to the south (area A-D, Plate SM1), and a pattern of alternating synforms and antiforms in the subsurface to the north (area E-G, Plate SM1).

In the Shublik and Sadlerochit Mountains, the pre-Mississippian sequence is composed mainly of thick-bedded to massive carbonates of the Katakturuk Dolomite, Nanook Limestone, and Mount Copleston Limestone (Dutro, 1970; Blodgett et al., 1992; Fig. SM2), which are thrust northward over Mississippian and younger rocks of the Ellesmerian sequence. The basement carbonate units display an intact internal stratigraphy, although they are low-grade metamorphic rocks with a conodont alteration index (CAI) of about 4 (Dumoulin and Harris, 1994). In limited areas in the northeastern Sadlerochit Mountains and northwestern Shublik Mountains the pre-Mississippian sequence also includes a poorly known basal unit composed mainly of metabasalt and meta-clastic rocks (unit "pCpu," Fig. SM2).

The Katakturuk Dolomite is at least 2500 m thick and is thought to be Late Proterozoic in age based on the presence of stromatolites, the lack of shelly fossils, and its stratigraphic position beneath the Nanook Limestone, of mainly Lower Paleozoic age, and above metabasalt that yields radiometric dates of roughly 700 and 800 Ma (Clough et al., 1990). The Katakturuk Dolomite has been subdivided into a number of map units, most of which are present in both the Shublik and Sadlerochit Mountains (Robinson et al.,

1989). To show this stratigraphy, we have grouped these internal units into lower, middle, and upper parts, designated "pCkI," "pCkII," and "pCkIII," respectively (Plate SM1; Fig. SM3).

The Katakturuk Dolomite is overlain unconformably by about 1200 m of Upper Proterozoic to Ordovician Nanook and Lower Devonian Mount Copleston Limestone, designated "DOCn" on our map and section (Fig. SM2, Plate SM1). These rocks are separated from overlying Mississippian strata of the Ellesmerian sequence by the sub-Mississippian unconformity. In the Sadlerochit and Shublik Mountains, the angular discordance across this unconformity ranges from 20 to 30 degrees, with the carbonate units of the pre-Mississippian sequence dipping to the south more steeply than the overlying Ellesmerian strata (Robinson et al., 1989).

South of the Shublik Mountains, the pre-Mississippian sequence is exposed in the Third and Fourth Ranges, at the southern end of our transect. In the Fourth Range it consists of partly recrystallized black limestone and phyllite and contains the trace fossil Planolites (R.B. Blodgett, oral communication, 2/2/98). Based on the presence of this trace fossil and the absence of shelly fossils, this unit is thought to be Upper Proterozoic and coeval with the unfossiliferous lower part of the Nanook Limestone (Blodgett, oral communication, 1998).

Following this correlation, we have designated a “Proterozoic to Lower Paleozoic?” unit in the upper part of the basement south of the Shublik Mountains (shown in medium gray, Plate SM1) to indicate rocks of similar age to the Katakturuk Sequence and Nanook Limestone.

Beneath the "Proterozoic to Lower Paleozoic?" unit we have inferred an older basement unit, designated "Proterozoic?” on Plate SM1. This unit is meant to encompass all rocks that underlie the Katakturuk Dolomite, possibly including age-equivalents of the Neruokpuk Quartzite which is exposed 10 km south of our section (Reiser et al., 1971). The “Proterozoic?” unit is not exposed in the area of our transect, so it should be considered speculative.

The nature of the basement north of the Sadlerochit Mountains is known from seismic lines AN84-6 and AN85-8 and, for the upper part of the basement, from exploratory wells in the area of Flaxman Island and the Canning River. Lithologies reported in these wells include argillite,

limestone, dolostone, quartzite, phyllite, and chert (Fisher and Bruns, 1987; Bird and Molenaar, 1987; Bird et al., 1987).

Recent, detailed studies of lithofacies in the wells at Flaxman Island and the adjacent islands to the west (Dumoulin, Chap. CC) indicate that the upper 400 m or so of the basement in that area is composed of an upper unit of sandstone and carbonate and a lower unit dominated by shale and siltstone. Both the upper and lower units have dips of less than 15°. The sandstones in the upper unit are not recrystallized, and the fine-grained rocks in the lower unit lack slaty cleavage, suggesting that the shallow part of the basement in this area has undergone less internal deformation than other parts of the pre-Mississippian sequence. Fossil fragments in the upper unit include phosphatic brachiopods and pelmatozoan debris, indicating that these rocks are Cambrian or younger. Based on these observations and on our seismic interpretation for the northern part of the cross-section, we have inferred a "Lower Paleozoic?" unit in the upper part of the basement in this area (Plate SM1).

The lateral extent of this "Lower Paleozoic?" unit was delineated on the basis of the seismic data in the northern part of the cross section (Plate SM1, area F-G). This area contains two broadly synformal areas with concave-up reflections that appear to flatten upsection and include internal unconformities. This pattern suggests that these are syntectonic basins that rest unconformably on older, more highly deformed basement rocks. They may be piggy-back basins formed in a contractional setting or large grabens formed in an extensional regime. Based on their geometric configuration and the nature of pre-Mississippian age structures observed farther south, we favor the piggy-back basin interpretation. In this case, the age of the sedimentary fill may date the pre-Brookian contraction that affected the basement in this area.

Beneath these synformal areas and in the remaining area beneath the coastal plain, we have inferred that the "Proterozoic to Lower Paleozoic?" and "Proterozoic?" successions are present, deformed in a simple fault-bend fold geometry. As in the area south of the Shublik Mountains, these units are meant to include age-equivalents of the Katakturuk Dolomite and Nanook Limestone and the rocks that underlie them. We have no direct information on the lithology or age of the deep basement in most of the area north of the Sadlerochit Mountains, so our interpretation in this area is highly speculative.

Ellesmerian Sequence

In the Shublik and Sadlerochit Mountains and the area to the south, the Ellesmerian sequence lies unconformably on the pre-Mississippian sequence and has a thickness on the order of 1000-1500 m. It is composed mostly of Upper Paleozoic to Early Mesozoic shallow marine sedimentary rocks thought to represent an ancient south-facing passive margin (present-day coordinates).

The Ellesmerian sequence includes the Kekiktuk Conglomerate and Kayak Shale of the Endicott Group (Mississippian, "Me," Plate SM1, Fig. SM3), the Alapah Limestone and Wahoo Limestone of the Lisburne Group (Mississippian and Pennsylvanian, "PMl"), the Sadlerochit Group, Shublik Formation, and Karen Creek Sandstone (Permian and Triassic, "TrPs"), the Kingak Shale (Jurassic-Early Cretaceous, "KJk"), and the Kemik Sandstone and pebble shale unit (Lower Cretaceous, included in "Ks") (Robinson et al., 1989). The Kemik Sandstone and pebble shale unit, although formally part of the Ellesmerian sequence, are located above the regional Lower Cretaceous Unconformity and are, therefore, included in our unit Ks, which encompasses all of the Cretaceous rocks above the unconformity (Plate SM1 and Fig. SM3).

North of the Sadlerochit Mountains, the thickness of the Ellesmerian sequence diminishes over a short distance by erosional truncation beneath the Lower Cretaceous unconformity, as has been documented in outcrops in the northeastern Sadlerochit Mountains (Mull, 1987; Robinson et al., 1989; Marsh Creek locality), in wells along the Canning River (Molenaar et al., 1986; Bird and Molenaar, 1987; Bird, Chap. GG) and in seismic images northwest of the Sadlerochit Mountains (Grow et al., Chap. NA). The position of the truncation limit of the Ellesmerian sequence in the area of our transect is not known precisely but probably is located between the Sadlerochit Mountain front and the south end of line AN84-6, in the region D-E in Fig. SM2 and Plate SM1a. Along seismic lines AN84-6 (E-F) and AN85-8 (F-G), the Ellesmerian sequence appears to be completely absent; one can see dipping reflections in the basement that are truncated by a regional unconformity (interpreted as the Lower Cretaceous unconformity) and onlapped or downlapped by clinoforms typical of the Brookian sequence. The seismic reflection signature that is typical of the Ellesmerian sequence (Potter et al., Chap. BD; Grow et al., Chap. NA) is absent.

Brookian Sequence

Our seismic stratigraphy interpretation of the Brookian sequence in seismic lines 84-6 and 85-8 (Plate SM1) follows that of Houseknecht and Schenk (Chap. BS), with facies interpretations based on well-correlation sections for the Canning River area west of our transect (Molenaar et al., 1986; Bird, Chap. GG).

Along our transect, the Brookian sequence is composed of Cretaceous and Tertiary foreland basin deposits, including condensed shale and interbedded bentonites of the Hue Shale (Lower to Upper Cretaceous) and turbidites and deltaic deposits of the Canning and Sagavanirktok Formations (Cretaceous to Tertiary).

For the purposes of the cross-section and kinematic models, we have divided these units according to age, e.g., "Ks," Cretaceous; "Tp," Paleocene; "Tel," Lower Eocene; "Teu," Upper Eocene; "To," Oligocene; and "Tplm," Miocene-Pliocene (Fig. SM3, Plate SM1). Age assignments were based on biostratigraphy from the Alaska State A-1 well at Flaxman Island, as reported by Poag (Chap. BI; Fig. SM4), and proprietary paleontological data from shot-holes along the south end of seismic line 84-6.

Units Ks and Tp are composed mainly of deep-water, shale-rich turbidites of the Canning Formation in the northern part of the coastal plain, with increasing amounts of deltaic clastics upsection and toward the south. These deposits are thought to represent a northeastward-prograding molasse-flysch sequence. They are overlain by "Tel," a shallow-water, transgressive marine shale unit known as the Mikkelsen tongue of the Canning Formation. The overlying units, Teu, To, and Tplm, are composed mainly of coarser-grained, deltaic facies of the Sagavanirktok Formation.

Implications for the timing of Brookian deformation, based on the stratigraphy of the Brookian sequence, will be discussed below in the section on the timing of deformation.

STRUCTURAL STYLE

Pre-Mississippian versus Brookian Age Structures

Two generations of structures have been recognized in the area of the transect: (1) structures involving basement rocks only, representing a pre-Mississippian deformational event, and (2) structures involving basement and overlying rocks of the Ellesmerian and Brookian sequences, a class of structures thought to represent Tertiary deformation associated with the Brookian orogeny.

In this study, we model only the sequential development of the Brookian-age structures. However, it is important to draw attention to the presence and style of pre-Mississippian age structures, because these older structures are thought to have played an important role in controlling the orientation of major faults activated during the Brookian orogeny (Kelley and Foland, 1987; Wallace and Hanks, 1990; Mull and Anderson, 1991).

Structures of Pre-Mississippian Age

Pre-Mississippian age structures have been recognized in exposures in the northeastern Brooks Range (i.e., Reed, 1968; Reiser and others, 1971, 1980; Oldow and others, 1987) and in seismic images of the region beneath the coastal plain (Fisher and Bruns, 1987). These structures are thought to pre-date the unconformity at the base of the Ellesmerian sequence (Reed, 1968; Wallace and Hanks, 1990; Mull and Anderson, 1991).

In outcrop, pre-Mississippian age structures are characterized by penetrative cleavage and folding of incompetent units, low-grade metamorphism, and regional faulting. In the subsurface in the area E-F-G of our cross section, where the Ellesmerian sequence is absent, pre-Mississippian age structures appear as a series of long-wavelength antiforms and synforms between about 4-7 km depth, truncated by the Lower Cretaceous unconformity (Plate SM1).

The deformation of the pre-Mississippian sequence has been referred to throughout northern Alaska as “pre-Mississippian” because it does not involve overlying Mississippian and younger rocks. However, in the northeastern Brooks Range relatively undeformed sedimentary rocks as old

as Middle Devonian overlie the penetratively deformed rocks of the pre-Mississippian sequence, suggesting that much of the basement deformation occurred prior to Middle Devonian time in this area (Anderson et al., 1994; Moore et al., 1994). This deformation may be associated with the Ellesmerian orogeny in the greater Arctic region.

It is believed that the Sadlerochit and Shublik Mountains uplifts represent thrust sheets that were originally juxtaposed during the Ellesmerian orogeny and later reactivated during the Brookian orogeny (Mull and Anderson, 1991; Rogers, 1992). This interpretation is based on structural and stratigraphic arguments. The structural argument is that Brookian structures in the pre-Mississippian sequence, such as the Weller Fault (Plate SM1), have an east-west strike that is co-planar with the structural grain in the basement rocks, suggesting an inherited structural fabric (Wallace and Hanks, 1990).

The stratigraphic argument is based on the repetition of similar pre-Mississippian stratigraphic units in the Sadlerochit and Shublik Mountains (Robinson et al., 1989). Along our line of section, most units in the Katakturuk Dolomite and lower Nanook Limestone are present in both ranges, and these successions are thought to have been repeated by faulting and subsequently beveled by erosion in pre-Mississippian time. We know of no field data that constrain the configuration of the fault that separates the two ranges, but it is thought to be either a north-dipping normal fault or a south-dipping reverse fault. We favor the second interpretation, because it fits kinematically with pre-Mississippian age contractional structures observed elsewhere. In addition, a north-vergent fault would be in a favorable geometry for reactivation during the Brookian orogeny. This inferred fault is shown in red at the base of the basement allochthon in the area B-C in our palinspastic restoration (Plate SM1b).

Extending this style of deformation northward, we have interpreted similar south-dipping thrust faults between basement blocks along the length of our palinspastic restoration (Plate SM1b). We show this ancient thrust system beveled flat beneath the sub-Mississippian unconformity, with a 20-30° difference in dip between the Ellesmerian and the underlying basement, in agreement with what is observed in the Sadlerochit and Shublik Mountains.

We have placed the basal detachment for the pre-Mississippian age thrust belt at a depth of 11-12 km (Plate SM1a); this is highly speculative and is

based on the geometry of the pre-Mississippian structures as interpreted from the seismic data beneath the coastal plain (Plate SM1a, area E-G).

Structures of Brookian Age

Brookian age structures involve rocks of the pre-Mississippian sequence and rocks of the overlying Ellesmerian and Brookian sequences. The style of Brookian age deformation is controlled in large part by differences in rheology in the stratigraphic sequence (e.g. Kelley and Foland, 1987; Wallace and Hanks, 1990; Wallace, 1993). The pre-Mississippian sequence in this area consists mainly of massive carbonates of the Katakturuk Dolomite and Nanook and Mount Copleston Limestones (Fig. SM3). These rocks behave rigidly and are interpreted to have deformed by regional-scale duplexing of thick coherent allochthons, rooted in a deep detachment horizon (Plate SM1a).

The Brookian sequence, in particular the Brookian flysch, is much less rigid than the pre-Mississippian sequence and deformed by thin-skinned, closely-spaced folds and faults above a detachment near the Lower Cretaceous unconformity. These small-scale structures are apparent in outcrop, but are mostly too small to resolve in the seismic data. In our cross-section, we have shown only the larger scale, seismically-imaged structures in the Brookian sequence (Plate SM1a).

The intervening Ellesmerian sequence, where it is present, is intermediate in structural competency between the Brookian sequence and the pre-Mississippian sequence. It consists of alternating intervals of structurally incompetent shale and relatively competent carbonate and sandstone. The competent intervals in the Ellesmerian sequence are much thinner than the massive carbonates in the pre-Mississippian sequence, so they form smaller-scale structures. The Lisburne Group carbonates, for example, deformed by short-wavelength detachment folding above a decollement in the Kayak Shale (Plate SM1; Wallace and Hanks, 1990; Wallace, 1993). Relatively competent layers of Kemik Sandstone, 30-40 m thick in this area (Knock, 1986, 1987; Mull, 1987), deformed by small-scale duplexing between a floor thrust in the Kingak Shale which underlies it, and a roof thrust in the Pebble Shale which overlies it (Plate SM1; Kelley and Foland, 1987; Meigs, 1989). We have shown the structures in the Ellesmerian sequence somewhat schematically because we are unable to display their smaller details at the scale of our cross-section.

Two regional detachment horizons allow for independent accommodation of shortening between the three main structural-stratigraphic domains described above: (1) a detachment in the Kayak Shale, i.e., near the sub-Mississippian unconformity, and (2) a detachment in shales (Kingak Shale, pebble shale unit, Hue Shale) near the Lower Cretaceous unconformity (Fig. SM3, Plate SM1a). In general, shortening in the Brookian sequence is rooted in the pebble shale-Hue Shale, shortening in the Ellesmerian sequence is rooted in the Kayak Shale detachment, and shortening in the pre-Mississippian sequence is rooted in an unknown decollement below the base of the Katakturuk Dolomite (Plate SM1).

In the case of the Kayak Shale detachment, it is important to point out that the Kayak thins northward and is absent in the northern part of the Sadlerochit Mountains (Kelley and Foland, 1987; Robinson et al., 1989; Wallace, 1993). North of the Kayak pinch-out, the carbonates of the Lisburne Group are found in depositional contact on the thick, competent carbonate rocks of the pre-Mississippian sequence (Katakturuk-Nanook succession). Thus, in the northern Sadlerochit Mountains, the Ellesmerian sequence deforms along with the underlying pre-Mississippian sequence, with no intervening detachment. In this area, the roof thrust for the basement duplex is in the upper part of the Ellesmerian sequence, as shown in Plate SM1a.

Basal Detachment Depth

We interpret the basal detachment for the Brookian age deformation to be at a depth of about 8-9 km below sea level south of the Sadlerochit Mountains, based on the thickness of the basement horses in the Shublik and Sadlerochit Mountains (3-4 km) and the depth to the autochthonous basement in the northern part of the transect as imaged in the seismic data (5 km deep). Restoring the top of the basement to 5 km places the base of the pre-Mississippian sequence at 8-9 km below sea-level. This is several kilometers deeper than the detachment depth presented in Wallace (1993), which was at a depth of about 5 km. That depth was based on the interpreted fault-bend fold geometry of horses in the pre-Mississippian sequence and an assumption that some additional thickening of the basement may have been accommodated on a second, deeper detachment not shown on his model.

In our interpretation, the basal detachment for the Brookian-age deformation terminates at a triangle zone, at kilometer 45 of the cross-section (Plate SM1).

Range-Front Structures

Two prominent faults on the cross section seem to depart from the basement duplex geometry described above. These are the Hue and Weller faults, which form the range-fronts of the Shublik and Sadlerochit Mountains, respectively (Plate SM1, Fig. SM2). Both faults cut upwards from the duplex in the pre-Mississippian sequence, through the Ellesmerian and Brookian sequences, rather than remaining confined beneath a roof thrust in the Kayak Shale or pebble shale-Hue Shale. We interpret these faults as young, out-of-sequence ruptures in an otherwise forward-propagating thrust sequence.

At both mountain fronts, these faults place Proterozoic rocks of the Katakturuk Dolomite over rocks as young as Paleocene. In detailed studies by Meigs (1989) and Rogers (1989; 1992), these structures were interpreted as late break-through structures developed in a fault-propagation fold regime. They would represent axial ruptures of oversteepened basement anticlines, which, prior to breakthrough, may have resembled the anticlines to the south of the Shubik Mountains (Plate SM1a, area A-B). This model is supported by the map pattern, which shows an along-strike transition from faulted anticlines in the high-relief areas, to simple, unbreached anticlines in the downplunge areas in both the Shublik and Sadlerochit Mountains (Robinson et al., 1989). Similar structures are present in the subsurface north and northeast of this cross section (Potter et al., Chap. BD).

STRUCTURAL AND STRATIGRAPHIC RESTORATION

Our palinspastic restoration (Plate SM1b) represents a structural and stratigraphic restoration of the cross section at a time just before the onset of the Brookian orogeny in this area. Based on arguments presented below, we believe the orogeny began in Middle Eocene time in this area, so our restoration represents a moment at the end of the Early Eocene. We have restored the regional-scale deformation associated with the Brookian orogeny and reconstructed the stratigraphy that we think was present in the mountains prior to their uplift and erosion (Plate SM1b). We use the Lower Cretaceous unconformity as the datum, flattened to horizontal.

Structural Restoration

We have restored Brookian-age thrust displacements of the pre-Mississippian sequence, large-scale thrust displacements in the lower part of the Brookian sequence, and large-scale detachment folding in the Ellesmerian sequence. We have not attempted to restore smaller-scale structures in any of the sequences, so the restoration should be considered as partial or minimum estimates. We believe the overall shortening in the Ellesmerian and Brookian sequences are roughly equivalent to the shortening in the basement, which we calculate below. Wallace (1993) compared the shortening in the basement duplex system with shortening in the Ellesmerian sequence in this area, and found them to be similar.

The basement duplex system was retrodeformed in two stages. First the youngest structures, the Hue and Weller Faults, were restored, resulting in simple anticlines beneath the Shubik and Sadlerochit Mountains. Second, the remaining displacements in the basement duplex were restored, starting with the fault beneath the Marsh Creek Anticline, and proceeding southward to the more internal faults. By this method, the top of the restored basement is approximately 104 km long, compared to 56 km for its present-day, deformed length (Plate SM1b). These measurements are taken from the frontal tip of the basement duplex, at kilometer 45, to the south end of the cross section (letter A, Plate SM1a). This represents the area that was shortened by Brookian deformation. The total shortening of the basement in our reconstruction is about 46% (Plate SM1b; (104-56km)/104km). This value exceeds that shown by Wallace (1993) in his cross section and restoration 7 km to the east. He shows about 36% shortening for the top of the basement, from the north end of his section to the north flank of the Fourth Range (Wallace, 1993, fig. 5).

The discrepancy between these shortening estimates is accounted for in part by an along-strike increase in the shortening in the Shublik Mountains between Wallace's section (1993) and this section because of breakthrough on the Hue Fault. Wallace's section is located in the eastern, downplunge part of the Shubliks, where breakthrough on the Hue Fault did not occur, whereas this section is located in the central Shubliks where breakthrough on the Hue Fault was significant. Additional differences arise from geometric differences between the two cross sections and the fact that our section

extends into the area beneath the Marsh Creek anticline, beyond the northern limit of the section by Wallace (1993).

The Ellesmerian sequence was restored along with the basement in the area north of the pinch-out of the Kayak Shale, i.e., where the Lisburne Group depositionally overlies basement with no intervening detachment. The northward termination of the detachment is denoted by the large black pin (Plate SM1a, area C-D) shown in the Sadlerochit Mountains. South of this pin, the Kayak Shale is present and the Ellesmerian sequence is detached from basement rocks, so it was retrodeformed independently, by unfolding of the large-scale detachment folds in the Lisburne.

Structures in the Brookian sequence are detached, for the most part, from both the basement and the Ellesmerian sequence. The Brookian sequence lies depositionally on inferred basement rocks in the undeformed area to the north, as indicated by the large black pin near kilometer 42 on the balanced cross section (Plate SM1a). South of this pin, we restored the regional-scale offsets within the Brookian sequence in the area of the Marsh Creek anticline.

Our seismic interpretation of the Marsh Creek anticline suggests some degree of linkage between the structures in the Brookian sequence and those in the underlying basement rocks (Plate SM1a, kilometer 40-60) in the area of our cross section. In fact, one fault cuts through the core of the basement expression of the anticline and upwards through the entire Brookian sequence, in the same style as the Weller and Hue Faults to the south. However, detailed analyses of seismic data in the down-plunge area of the Marsh Creek anticline farther east have led to the interpretation that the part of the anticline that involves the Brookian sequence is detached from the underlying basement deformation in that area (Potter et al., Chap. BD). Therefore we have restored the deformation in the Brookian sequence separately from that in the pre-Mississippian sequence where our transect crosses the Marsh Creek anticline.

Stratigraphic Restoration

We have tried to reconstruct thicknesses for the stratigraphic units in Brookian sequence prior to the onset of deformation in this area, that is prior to Middle Eocene time, based on the thermal maturities observed in rocks of the Ellesmerian sequence in the Shublik and Sadlerochit Mountains. We

used the conodont alteration indices (as reported in Johnsson et al., 1992) to deduce a maximum burial temperature for these rocks, then converted this temperature to an approximate burial depth, using an average geothermal gradient of 30°C/km.

A gradient of 30°C/km represents an average modern-day gradient calculated from corrected bottom hole temperatures in wells along the Canning River and near the coast (Nelson et al., Chap. WL). Geothermal gradients interpreted from vitrinite reflectance values in the same wells tend to be lower (Nelson et al., Chap. WL and Bird, Chap. VR) and may indicate a lower geothermal gradient existed in this area in the geologic past. This possibility should be kept in mind in the burial estimates that follow; a lower geothermal gradient would require a correspondingly greater depth of burial than what we present here.

Theoretically, vitrinite reflectance values of rocks at the surface can be used in the same way, but in the area of our transect, we found that surface vitrinite values varied widely, even from rocks in the same general outcrop area and in some cases from the same stratigraphic unit. Given this high degree of variability, we found it difficult to estimate paleotemperature and burial depth using surface vitrinite reflectance values.

Conodont alteration indices (CAI's) are shown at three locations along the top of the cross section (Plate SM1a): one on the south side of the Sadlerochit Mountains (at kilometer 76), a second on the south side of the Shublik Mountains (at kilometer 86), and a third on the north flank of the Fourth Range (at kilometer 100), near the south end of our transect. Each of these is an average value, based on a cluster of about 5 samples at each location, from a stratigraphic level near the base of the Lisburne Group. The three sample locations are restored to their retrodeformed positions in Plate SM1b, where they are used to estimate burial depth.

In the Sadlerochit Mountains area, the average CAI for the basal Lisburne Group is 3-4 (Plate SM1b, kilometer 102), corresponding to paleotemperatures of about 210°C (Rejebian et al., 1987; Bird, Chap. VR). Assuming a geothermal gradient of 30°C/km, this corresponds to a total burial depth of about 7 km for the lower part of the Ellesmerian sequence. If the thickness of the Ellesmerian sequence is taken as approximately 1.5 km,

an eroded Brookian section about 5.5 km thick can be estimated to have been present in the area of the Sadlerochit Mountains.

In the Shublik Mountains, the basal Lisburne has an average CAI of 4 (Plate SM1b, kilometer 118), corresponding to paleotemperatures on the order of 225°C. Assuming a paleothermal gradient of 30°C/km, 7.5 km of total burial for the basal Lisburne Group is estimated in that area.

In the Fourth Range, the basal Lisburne samples have an average CAI of 4-5 (Plate SM1b, kilometer 142), corresponding to paleotemperatures of about 250°C. Assuming the 30°C/km gradient, 8.3 km of total burial for the basal Lisburne Group can be estimated in that area.

These burial depths are only estimates, and probably carry a margin of error of +/- 2 km when all of the attendant uncertainties are considered-- such as the time-dependence of thermal maturation and the paleothermal gradient. However, the relative increase in calculated burial depth toward the south is quite certain and probably represents the combined effects of greater foreland basin flexure and, to a lesser extent, greater passive-margin subsidence in the southern part of the transect area prior to uplift and erosion during Brookian deformation.

TIMING OF DEFORMATION

The structural and stratigraphic restoration described above and shown in Plate SM1b provides the geometric basis for the kinematic modeling that we performed with Thrustpack. The other important ingredient is timing.

Timing of Thin-skinned Structures

Thin-skinned deformation in the Ellesmerian and Brookian sequences is an important part of the tectonic history of the transect area. Although its scale is too small to include in our Thrustpack modeling, we present a brief discussion here of its timing relative to the basement-involved structures.

Thin-skinned deformation in the Ellesmerian and Brookian sequences pre-dates some of the basement-involved structures, based on cross-cutting relationships in the Shublik and Sadlerochit Mountains and adjacent areas (Bader and Bird, 1986; Robinson et al., 1989; Wallace and Hanks, 1990). Thin-skinned anticlines with east-northeast trends, such as the anticline in

the Ellesmerian sequence in front of the northeastern Sadlerochit Mountains, are in some cases truncated by basement-involved uplifts with a more east-west trend, such as the main axes of the Shublik and Sadlerochit Mountains (Fig. SM2). These structural relations suggest a progression from thin-skinned to thick-skinned deformation in some locations.

In the Marsh Creek area directly north of the eastern Sadlerochit Mountains, 32 km east of our cross section, Mull (1987) and Kelley and Foland (1987) documented multiple thrust repetitions of the Kemik Sandstone. Kemik facies in these thrust sheets are similar to Kemik facies more than 10 km to the south, on the south side of the Sadlerochit Mountains. The apparent northward displacement of these facies has been used as evidence for an early stage of thrusting along a detachment in the Kingak Shale prior to formation of the basement-involved structures in the Sadlerochit Mountains (Mull, 1987).

In addition to thin-skinned thrusting of the Kemik Sandstone in the Sadlerochit Mountains area, thrust emplacement of allochthonous facies of the Hue Shale and Canning Formation has been proposed in the Arctic Creek area on the south side of the eastern Sadlerochit Mountains, 38 km east of our transect. Mull and Decker (1993) described allochthonous facies of the Hue Shale and Canning Formation of the lower Brookian sequence that contrast markedly with coeval rocks to the west in Ignek Valley, between the Sadlerochit and Shublik Mountains. Similar facies are present southwest of the Canning River and are inferred to be part of the same allochthonous sheet as in the Arctic Creek area. The regional evidence suggests that these rocks were emplaced across the area before formation of basement-involved structures in the Sadlerochit and Shublik Mountains.

Some of the thin-skinned deformation in the Ellesmerian and Brookian sequences, including the intricate duplexing of the Kemik Sandstone, may have occurred prior to development of basement-involved structures such as the Shublik and Sadlerochit Mountains anticlines. However, we suggest that the amount of time that elapsed between development of thin-skinned and thick-skinned structures was not great. It is likely that the the observed pattern represents a natural downward progression in detachment level through time, as is common in fold and thrust belts (Suppe, 1985).

Timing of Basement Deformation

In our kinematic modeling, we have focussed on the development of the basement duplex system, because it is this deeply-rooted fault system that is responsible for most of the vertical relief in this area, and therefore the main agent in producing uplift, erosion, and cooling of rocks in the thrust belt. We have used two main lines of evidence to infer the absolute timing of the deep-seated Brookian deformation in the transect area: (1) stratigraphic evidence from the foreland basin, and (2) structural and thermal evidence from the thrust belt. The main lines of evidence are summarized in Fig. SM5.

Starting with the foreland basin, i.e., the area north of the Sadlerochit Mountain front, Cretaceous and Paleocene are represented by thick deposits of molasse and flysch that prograded northeastward from a southern or southwestern source area (Fig. SM5, upper part; Bird, Chap. GG). These are overlain by Lower Eocene transgressive marine shales. The depositional environment in the foreland basin area changed in Middle Eocene time, when a regional unconformity developed, followed by shallow-water conditions and the accumulation of mainly molasse-type deposits for most of the remaining the Tertiary.

The onset of local deformation in the foreland basin area was in the Late Oligocene, according to our seismic interpretation of the north flank of the Marsh Creek anticline. In that area, we see progressive unconformities of Late Oligocene age, and overlying Lower Miocene strata are more gently tilted (km 50, Plate SM1a). Potter and others (Chap. BD) report "fanning reflections" from late Oligocene to Early Miocene strata in the same area, presumably also representing progressive uplift of the Marsh Creek anticline during accumulation of those strata. From these observations we surmise that the foreland basin area in the northern part of our transect underwent southward flexure in Cretaceous and Early Tertiary time, followed by possible uplift and erosion in mid-Eocene time, and finally local erosion and deformation associated with the development of the Marsh Creek anticline in Late Oligocene to Early Miocene time.

Thick deposits of flysch and/or molasse were also accumulating in the thrust belt in the southern part of our transect during Cretaceous, Paleocene, and early Eocene time (Fig. SM5, lower part). According to our stratigraphic

reconstruction, described above and shown in Plate SM1b, these deposits were thickest in the southern part of the transect.

Although the duration of deposition in the thrust belt is not known, we believe that it had ended by mid-Eocene time and is reflected in the first major cooling episode recorded by apatite fission-track ages from the area of the Shublik and Sadlerochit Mountains (ca. 45 Ma; O'Sullivan, 1993; O'Sullivan et al., 1993). These Middle Eocene cooling ages have been interpreted as a consequence of rapid uplift and erosion associated with contractional deformation (O'Sullivan, 1993, 1994; Hanks et al., 1994). In this paper, we suggest that these ages relate specifically to the basement duplexing that resulted in the creation and erosion of major anticlines in the Sadlerochit and Shubik Mountains.

A later episode of cooling affected the thrust belt in Late Oligocene time according to a second population of apatite fission-track ages from the thrust belt (ca. 23 Ma; O'Sullivan, 1993, 1994; Hanks et al., 1994). The timing of this cooling event is similar to the age of the syndepositional strata on the north flank of the Marsh Creek anticline. These cooling ages probably relate to a renewed period of basement faulting resulting in deeper erosion in the Shublik and Sadlerochit Mountains and propagation of the basement duplex into the area of the Marsh Creek anticline.

A third episode of deformation, not recorded by fission-track ages, occurred in the northern part of the transect area in Miocene to Recent times. The primary evidence for this event comes from the presence of young geomorphic features and recent seismicity in the Sadlerochit Mountains and adjacent areas of the coastal plain and offshore area to the north (Grantz et al., 1983; Bader and Bird, 1986; Grantz et al., 1987; Kelley and Foland, 1987; Robinson et al., 1989). Recent to active geomorphic features include (1) uplifted and tilted Pleistocene terraces and fans on the coastal plain and in the Sadlerochit Mountains (Carter et al., 1986; Burbank et al., 1996), (2) folded Pliocene strata in the axial part of the Marsh Creek anticline (Bader and Bird, 1986), (3) antecedent streams that cut from south to north across the Sadlerochit Mountains, including the Katakturuk and Itkilyariak Rivers (e.g., Burbank et al., 1996), (4) low-sinuosity range fronts with triangular facets and freshly incised streams along both the Shublik and Sadlerochit Mountain fronts (Bader and Bird, 1986; Robinson et al., 1989), and (5) folds and fault scarps, involving Holocene deposits in some locations, in the offshore area north of our transect (Grantz et al., 1983).

The age range of these features is assumed by most experts to be Late Neogene to Recent, and the seismic activity is ongoing. We interpret these features and the associated seismic activity to be manifestations of late stages of contraction associated with the Brookian orogeny. The first author, Cole, believes that the very young geomorphic features and active seismicity in the Shublik and Sadlerochit Mountains are related to Pleistocene to Recent displacements on the Hue and Weller Faults.

Summary of Timing Constraints

Merging the available evidence, from the foreland basin and the fold and thrust belt, we suggest four main stages of basement-involved Brookian deformation in the area of our transect: (1) Cretaceous to Early Tertiary flexural subsidence from tectonic loading south of our transect, (2) Middle Eocene growth of the basement duplex in the southern part of the transect (3) Late Oligocene to Early Miocene renewed thrusting as the basement duplex system propagated northward, and (4) Miocene to Recent tectonic activity, possibly related to displacements on the Hue and Weller faults.

A FORWARD MODEL

Based on the timing constraints discussed above and shown in Fig. SM5, and on the structural and stratigraphic restoration shown in Plate SM1b, we created the following forward model with Thrustpack to illustrate the major stages of deposition and basement-involved deformation along this transect (Fig. SM6). We specified values for both the magnitude and timing of displacement on each fault in the model, and made adjustments to attain a final model geometry that resembled the original balanced cross section. The final set of values that we used as input is given in Table SM1.

Thrustpack computes the successive stages of deformation using an algorithm that simulates fault-bend-fold geometry and kinematics (Suppe, 1983). With this algorithm, layer thicknesses and lengths remain constant, and folding takes place by flexural slip between layers. For further information on the workings of the computer model, see Sassi and Rudkiewicz (1996).

The numerical time window for each tectonic and/or sedimenation event is an estimate based on time scales of Gradstein and others (1994) and

Berggren and others (1995). For the timing of depositional events in the foreland, we follow the timing used by Rowan (1997) in her basin modeling along the Canning River. Each bounding numerical age should be considered to carry an uncertainty on the order of 5 Ma, largely because of uncertainties in the ages of the rock units. However, we believe the relative timing of these events is well-constrained, based on the timing arguments presented above and shown in Fig. SM5.

Figure SM6 shows the sequential stages of the kinematic model. In each stage, basement rocks are shown in gray, except for basement rocks in the Sadlerochit and Shublik Mountains, which are highlighted in brown. Colors for the stratigraphic units in the Ellesmerian and Brookian sequences correspond to those in Plate SM1. The yellow plus symbols represent "history points," used in the Thrustpack program to track the thermal history of source rocks in the Shublik Formation during successive stages of sedimentation and deformation.

State 1, 130 Ma (Early Cretaceous). This is the initial state of the kinematic model and represents a cross-sectional view of the transect area in Early Cretaceous time (Fig. SM6A). The upper surface of the model represents the Lower Cretaceous unconformity (LCU), and the blue, pink, and dark green units comprise the Ellesmerian sequence, deposited on an earlier south-facing passive margin. Note that the Ellesmerian sequence is absent by erosional truncation north of about kilometer 88.

State 2, 65 Ma (End Cretaceous). This state is a snapshot at the end of the Cretaceous (Fig. SM6A). We have shown southward flexure of the former passive margin due to tectonic loading south of the area of the transect and the accumulation of about 2.5 km of Cretaceous deposits above the Lower Cretaceous unconformity in the southern part of the model. The thickness of the Cretaceous deposits tapers to zero in the northern part of the model. The model-simulated deposits correspond to unit Ks in the coastal plain and include the Kemik Sandstone, pebble shale unit, and Hue Shale in the lower part, and mainly the thick Cretaceous shales of the Canning Formation (Plate SM1).

State 3, 55 Ma (End Paleocene). This state is a snapshot at the end of the Paleocene (Fig. SM6A). We have simulated additional southward flexure and deposition of a northward-tapering wedge of Paleocene deposits, with a maximum thickness of 2.5 km in the southern part of the model. In the

coastal plain area, these deposits correspond to shales and sandstones in the Paleocene part of the Canning Formation (Bird, Chap. GG), shown as unit Tp in Plate SM1.

State 4, 47 Ma (Early to Middle Eocene). This state is a snapshot at the beginning of the Middle Eocene (Fig. SM6B). We have simulated deposition of Early Eocene shales, unit Tel (Plate SM1), which includes the Mikkelsen tongue of the Canning Formation in the coastal plain. This unit is thought to represent a regional marine transgression (Bird, Chap. GG) that occurred prior to the onset of basement-involved deformation in the immediate area of our transect. This is the time of maximum burial for rocks in the southern part of the transect, i.e., south of about kilometer 80 (Fig. SM6B).

State 5, 37 Ma (End Middle Eocene). This state is a snapshot at the end of the Middle Eocene (Fig. SM6B). It shows the first episode of basement-involved deformation and deep erosion of rocks along our transect, by growth of a large basement duplex south of about kilometer 80. The basement-involved deformation was accomplished by shortening totalling 30 km on faults 1-4 (Table SM1; Fig. SM6b) accompanied by coeval erosion of up to 3 km of Cretaceous and Tertiary deposits in the Sadlerochit and Shublik Mountains and the area to the south. Erosion of this magnitude is required to produce the mid-Eocene apatite fission-track ages in the Sadlerochit and Shublik Mountains. A regional mid-Eocene unconformity recognized in the coastal plain area may be related to this episode of deformation and denudation in the mountains.

We have not modeled the internal shortening in the Ellesmerian and Brookian sequences in this or subsequent states, only passive folding of the cover units above the basement duplex. Therefore the effects of tectonic thickening of these units is not considered in our model.

State 6, 34 Ma (End Late Eocene). This state is a snapshot at the end of the Late Eocene. We have simulated deposition of Upper Eocene strata north of the newly formed basement duplex, e.g., north of about kilometer 80 (Fig. SM6B). These deposits correspond to the Sagavanirktok Formation in most of the coastal plain area and to deeper water deposits of the Canning Formation near Flaxman Island and in the offshore region.

State 7, 32 Ma (Early Oligocene). This state is a snapshot of the Early Oligocene (Fig. SM6C). We have simulated deposition of the Lower Oligocene unit To (Plate SM1) north of about kilometer 70 during this period of apparent tectonic quiescence.

State 8, 22 Ma (Early Miocene). This state is a snapshot of the Early Miocene (Fig. SM6C). We have simulated renewed basement-involved thrusting during Middle Oligocene to Early Miocene time with 15 km of total shortening on faults 5 and 6. These displacements produced a second stage of uplift in the Shublik and Sadlerochit mountains and initial formation of the Marsh Creek anticline. We have eroded the top of the Marsh Creek anticline, and invoked a second period of erosion in the Sadlerochit and Shublik Mountains allochthons and the area to the south, to account for the Oligocene fission-track ages in that area.

State 9, 0 Ma (Present-day, uneroded). This state represents the present-day geometry of the transect area (Fig. SM6C). We have simulated deposition of the unit Tplm, which represents all of the remaining Miocene and Pliocene sedimentary rocks in the northern part of the transect (Plate SM1). We have also shown high-angle breakthrough structures in the cores of the Shublik and Sadlerochit Mountains anticlinoria at this time, via young displacements on the Hue and Weller Faults (faults 7 and 8, Fig. SM6C). These final fault displacements result in an additional 3 km or so of shortening. We have not simulated erosion for this final kinematic state, in order to show the geometry and scale of displacement on the high-angle breakthrough structures.

THERMAL MODEL

Thermal modeling was conducted with Thrustpack to track the thermal history of all the rocks in the model as well as the specific maturation history of oil-prone source rocks in the Shublik Formation. The results of the thermal modeling serve as a check on the internal consistency of the kinematic scenario, as well as providing predictions for timing of source rock maturation with respect to sedimentation and deformation events.

Using Thrustpack we can compute the thermal structure in two dimensions for each kinematic state, taking into account heating and cooling of rocks driven by sedimentary burial, tectonic transport, and erosion. The thermal computations also take into account changes in the surface temperature at

the top of the model, and heat flow at the base of the model. In this study, we assumed a constant heat flow at the base of the model of 55 mW/m^2 (at a depth of 20 km), which is within the range 52-62.5 mW/m^2 suggested by Rowan (1997). We also relied on Rowan's (1997) estimates for surface temperatures during each kinematic state (Table SM1). The transfer of heat through the rocks was assumed to occur by pure conduction, using the standard two-dimensional heat equation, solved for a finite-element mesh.

Thrustpack offers a set of standard lithologies with default material properties that can be selected by the user to approximate the thermal properties for each layer in the model. We used the lithologies and default thermal properties shown in Fig. SM7. Thrustpack accounts for changes in porosity and permeability in each layer as a function of burial depth, following an empirical porosity-vs.-depth curve for the selected standard lithology. However, changes in layer thickness due to compaction are not modeled in Thrustpack (Sassi and Rudkiewicz, 1996).

Using Thrustpack it is also possible to compute maturation histories for kerogen and vitrinite, using a set of typical kinetic properties for these materials. The kinetic parameters and equations are given in Sassi and Rudkiewicz (1996). The user is given the choice of modeling Type I, Type II, or Type III kerogen and/or vitrinite in one or more stratigraphic layers in the model. In this study, we modeled Type II kerogen in the pink layer ("TrPs"), which contains the Shublik Formation, to track the maturation of this source rock through each stage of sedimentation and deformation.

We also tracked the thermal evolution of rocks in the Ellesmerian and Brookian sequences in terms of vitrinite reflectance, or Ro. The vitrinite reflectance modeling yields results that can be readily compared with measured Ro values along the transect and in nearby wells (Bird et al., Chap. VR). This serves as a check on whether the thermal modeling results are in agreement with observed thermal maturity.

Finally, we selected "history points" at three locations within the Shublik Formation, as shown by yellow plus signs in Fig. SM6. Thrustpack computes a complete thermal and maturation history at each of these points, which can be used to discern spatial variations in both timing and degree of thermal maturation. Two of these history points were placed at locations where we have independent thermal history predictions from apatite fission-

track modeling, in Ignek Valley and at the front of the Sadlerochit Mountains.

Results of Thermal Modeling

First we compare the thermal predictions of the model with measured temperatures and paleo-temperature estimates. Then we present the model-predicted maturation history for the Shublik Formation, in terms of both vitrinite maturation and kerogen transformation. Finally we discuss possible implications for the timing and extent of petroleum generation in the transect area.

Modern and Ancient Thermal Gradients

Downhole temperatures from wells on Flaxman Island serve as a field check on the present-day isotherms predicted by our model. Figure SM8 shows, in blue, a regression line fitted to the corrected bottom-hole temperatures in the Alaska State D-1 well. The corrected temperatures were calculated from observed temperatures reported in Nelson and others (Chap. WL). The red line is the predicted temperature profile for this location using thermal modeling with Thrustpack. The overall gradient predicted with Thrustpack is close to the observed gradient. The mismatch at the top of the profiles is due to the fact that we did not include a permafrost layer in the Thrustpack model. Other differences in the profiles could probably be corrected by adjusting the model input values for thermal conductivities. However, for the purpose of obtaining first-order, regional predictions, we believe the fit is reasonably close. The predicted gradient is roughly 25°C/km, while the observed gradient is roughly 30°C/km.

In a similar way, we can compare predicted-vs.-observed vitrinite reflectance profiles at the Alaska State D-1 well. Vitrinite reflectance increases as rocks are heated and records the maximum temperature that they attain. Because the reflectance value is proportional to temperature, it can be viewed as a proxy for the ancient thermal gradient. Figure SM9 shows the observed vitrinite reflectance values for the Alaska State D-1 well (from Bird, Chap. VR), compared to model-predicted Ro values for a corresponding location, at a stratigraphic level near the base of the Brookian sequence. The predicted Ro values are in excellent agreement with the observed values for this location, suggesting that our thermal modeling produces realistic paleo-thermal predictions at this location.

Thermal History of Shublik Formation

In Fig. SM10 we present thermal history plots for three history points selected in the Shublik Formation. Point 1 is in a location on the south flank of the Shublik Mountains, Point 2 is in Ignek Valley, and Point 3 is at the Sadlerochit Mountain front. They represent a spread of roughly 20 km along the final cross section. The thermal history plot starts at the beginning state of the kinematic model, at 130 Ma (Early Cretaceous), and shows successive temperatures experienced at these locations through time.

Points 1 and 2 start at higher temperatures than Point 3 because of deeper burial beneath the southward-thickening Kingak Formation, which was present during kinematic state 1 (Fig. SM6a). All three points undergo progressive heating during deposition of the Cretaceous, Paleocene, and lower Eocene units (Ks, Tp, and Tel; States 1, 2, and 3), followed by two cooling episodes, one in the Middle Eocene and the second in the Middle to Late Oligocene, corresponding to uplift and erosion during kinematic states 6 and 9 (Fig. SM6), respectively. The Middle Eocene cooling episode is more extreme at points 1 and 2, where erosion was greater. Point 3 experienced deeper erosion, and therefore more extreme cooling, during the Oligocene event.

Comparisons with Fission-track Modeling

In Figs. SM11 and SM12, we compare the thermal histories that we generated with Thrustpack for history points 2 and 3 with results of thermal modeling of fission-track samples in Ignek Valley and the Sadlerochit Mountain front, respectively (O'Sullivan, 1993; O'Sullivan, 1994; O'Sullivan et al., in prep). We made a similar comparison at the north end of our cross section, at kilometer 7, to check with O'Sullivan's thermal modeling for the Alaska State C-1 well (O'Sullivan, 1993; Fig. SM13). The locations of the apatite fission-track samples are shown in Plate SM1a.

For history point 2, which corresponds to the Ignek Valley fission-track sample locality, a thermal history comparison is shown in Fig. SM11. The blue curve is based on fission-track samples from Cretaceous rocks, whereas the red curve is based on our history point in the Shublik Formation. Two cooling events have been modeled to explain the fission-track ages, the first event at about 45-40 Ma, and a second at 35-30 Ma (O'Sullivan, 1993;

O'Sullivan, 1994). Similar age events are predicted by the Thrustpack modeling, the first at 47-37 Ma, and a second one at 32-22 Ma. The agreement between the two models seems quite close, considering that the uncertainties on these ages are of the order of +/- 5 Ma.

Figure SM12 shows a thermal history comparison for the Sadlerochit Mountain front. The fission-track modeling in this area is based on data from Triassic age rocks near the mountain front (sample no. 91POS77 in O'Sullivan), and the Thrustpack result is based on history point 3, in Triassic rocks of the Shublik Formation. The fission-track modeling indicates two cooling ages in this area, one at 50-45 and the other at 30-25, with the possibility of a third event after 25 Ma (Fig. SM12). The Thrustpack model predicts events with a similar magnitude of cooling, and similar timing, again at 47-37 Ma, and 32-22 Ma.

Figure SM13 compares thermal histories for a location at the north end of our cross section, corresponding to fission-track samples from the Alaska State C-1 well. According to the fission-track modeling, this area underwent continuous heating until 25 Ma, followed by a small amount of cooling from 25-15 Ma, and then resumed heating. The predicted thermal history for this area, according to our Thrustpack modeling, is similar, and the final temperatures from the two methods are in good agreement.

Maturation in Terms of Vitrinite Reflectance

We can also view the progressive vitrinite maturation of these history points (Fig. SM14) through time. Maturation occurred slowly during Cretaceous time, during deposition of the Hue and lower Canning Formations. Maturation accelerated in the Paleocene (65 Ma), during rapid deposition of the Paleocene and Lower Eocene units. Maximum burial was reached by 45 Ma in the south, and several millions of years later in the north. This northward transgression of maximum burial age reflects the northward progression of deposition and deformation into the foreland basin.

According to these results, the Shublik Formation matured rapidly in Paleocene to Eocene time, mainly due to sedimentary burial beneath the Lower Tertiary turbidites. By middle to late Eocene time, the Shublik at history point 1 and the area to the south had attained Ro values in excess of 2.0, suggesting that it had probably generated all of its hydrocarbons by that time in the southern part of the model. If the model predictions are correct,

then the southern area of the Shublik generated its oil prior to the development of major structures in this area.

Figure SM15 shows the contoured vitrinite reflectance predicted by the model for two important kinematic states-- I) at the end of the Early Eocene (state 4, Fig. SM6), during maximum burial, and II) at the end of the Pliocene (state 9, Fig. SM6), in the final Thrustpack state. Vitrinite reflectance, shown in a spectrum of colors from blue to red, is superimposed on the stratigraphy, which is shown by thin black lines. This diagram illustrates the important decrease in vitrinite reflectance from south to north, within a given stratigraphic horizon in the Ellesmerian or Brookian sequence. Vitrinite reflectance in the Shublik Formation, with the selected history points shown again here, decreases from Ro>2 in the southern part of the section (Fig. SM15, part I, kilometer 150) to Ro<1 near the truncation limit of the Shublik at the northern end of the section (Fig. SM15, part I, kilometer 100). The relatively low thermal maturity in the north raises the possibility for ongoing oil generation after mid-Eocene time from the Shublik Formation in the northern part of the transect.

Transformation Ratio of Shublik Kerogen

Finally, we show the predicted oil generation from the type II kerogen in the Shublik Formation, again in terms of the selected history points (Fig. SM16). According to our model, all three history points moved through "Peak Oil Generation" during deposition of the Paleocene flysch unit ("Ps") between 65-55 Ma. According to our kinematic scenario, this is about 10 Ma before the onset of basement-involved thrusting in this area and probably predates development of any sizable structural traps. However, there is a possibility that the small wedge of Shublik Formation north of history point 3 underwent peak oil generation after the initiation of the deformation. There is also potential for stratigraphically higher source rocks, such as the Hue Shale and Mikkelsen Tongue of the Canning Formation, to have generated oil after major structural traps had formed.

Considering that the bulk of the Shublik was generating its oil in Paleocene time, we can examine the kinematic states for this period (Fig. SM6, States 2 and 3) to estimate the probable migration direction for that oil. In States 2 and 3 the Shublik Formation has a definite southward dip, suggesting that migration at that time would have been toward the north, presumably toward the area where it is truncated by the Lower Cretaceous unconformity.

After deformation started, in Middle Eocene time, the northern part of the Shublik, north of history point 2 (Fig. SM6, States 5-10), reversed to a northward dip. This suggests that oil generated from this small wedge of Shublik probably migrated southward toward the structural high associated with the Shublik and Sadlerochit Mountain uplifts.

DISCUSSION

According to our model for the kinematic and thermal history of this part of the northeastern Brooks Range, source rocks in the Shublik Formation had matured by Early Eocene time, before the onset of deformation in this area. This suggests that contractional structures in this region are poor exploration targets for petroleum derived from the Shublik source. Stratigraphic targets are more prospective, particularly in the northern part of the transect, because the migration direction was probably toward the north during Paleocene time, when the main area of the Shublik Formation was generating oil. Most of the Brookian sequence in this area is composed of shaly turbidites, becoming more distal toward the north, so the Ellesmerian sequence may be a more promising section for finding a suitable reservoir for the Paleocene oil.

The small wedge of Shublik Formation that is thought to be present to the north side of the Sadlerochit Mountain front may have generated oil after the Paleocene, and perhaps after the formation of contractional structures associated with the Brookian orogeny. Oil generated after the onset of deformation would probably have migrated southward, into the area of the Shublik and Sadlerochit Mountains structural high. Uplift and deep erosion of that structural high makes it an unfavorable trap.

We did not model the maturation of younger source rocks in this area, namely the Hue Shale and the Mikkelsen Tongue of the Canning Formation. Those units are higher in the stratigraphic section, so their timing of maturation was certainly younger and therefore more favorable for charging structural traps formed during the Brookian orogeny.

CONCLUSIONS

Integrating structural data from the Sadlerochit and Shublik Mountains area with structural and stratigraphic data from the adjacent coastal plain, we

created a regional balanced cross section extending from the thrust belt into the foreland basin. Based on fission-track ages, cross-cutting relations, and ages of syntectonic sediments, we have interpreted the major episodes of deformation and sedimentation along this transect and incorporated them into a kinematic model that shows sequential stages of the geologic history from Early Cretaceous time to the present.

The kinematic history is characterized by southward flexure and foreland basin sedimentation in Early Cretaceous to Early Eocene time, followed by the onset of basement duplexing in Middle Eocene time, and renewed thrusting and northward propagation of the duplex system into the area of the Marsh Creek anticline by Middle to Late Oligocene time. The final stage of our kinematic model shows young thrust break-through of the Shublik and Sadlerochit Mountains anticlines to produce the modern range-fronts and the intervening Ignek Valley.

The thermal history of rocks in the Ellesmerian and Brookian sequences in the area of the Shublik and Sadlerochit Mountains began with progressive heating during sedimentary burial in Early Cretaceous to Early Eocene time, followed by episodic cooling in Middle Eocene and Oligocene time, and possibly a third cooling episode in Miocene to Recent time, not recorded by fission-track ages. Rocks in the foreland basin, north of the Marsh Creek anticline, had a simpler thermal history, characterized by ongoing, progressive heating from the Early Cretaceous time to Recent times.

Shublik Formation oil source rock maturation occurred mainly before the initiation of the Brookian structures and probably generated oil during Paleocene to Early Eocene time. Because of the regional southward flexure in the transect area at that time, migration was probably toward the north, i.e., toward the distal part of the foreland basin.

The northernmost wedge of the Shublik Formation may have generated oil later, perhaps in the Middle Eocene after deformation had begun to uplift the Shublik and Sadlerochit Mountains. Oil generated from the Shublik Formation in Middle Eocene time or later probably migrated southward into the newly formed Shublik-Sadlerochit structural high. Our results for the Shublik Formation suggest that the stratigraphically higher source rocks could have generated oil after formation of structural traps associated with the Brookian orogeny.

ACKNOWLEDGMENTS

This study would not have been possible without the cooperation and financial and logistical support from the Institut Français du Pétrole to use their Thrustpack modeling program. We also thank Tom Moore and Chris Potter for providing careful and insightful reviews of the manuscript.

REFERENCES

Anderson, A.V., Wallace, W.K., and Mull, C.G., 1994, Depositional record of a major tectonic transition in northern Alaska: Middle Devonian to Mississippian rift-basin margin deposits, upper Kongakut River region, eastern Brooks Range, Alaska, in Thurston, D., and Fujita, K., eds., 1992 Proceedings International Conference on Arctic Margins, U.S. Minerals Management Service Outer Continental Shelf Study 94-0040, pp. 71-76.

Bader, J.W., and Bird, K.J., 1986, Geologic map of the Demarcation Point, Mt. Michelson, Flaxman Island, and Barter Island quadrangles, Alaska: U.S. Geological Survey Miscellaneous Investigations Map I-1791, scale 1:250,000, 1 sheet.

Berggren, W.A., Kent, D.V., Swisher, C.C., and Aubry, M-P, 1995, A revised Cenozoic geochronology and chronostratigraphy: SEPM (Society for Sedimentary Geology) Special Publication No. 54.

Bird, K.J., and Molenaar, C.M., 1987, Stratigraphy, in Bird, K.J., and Magoon, L.B., eds., Petroleum Geology of the northern part of the Arctic National Wildlife Refuge, northeastern Alaska: U.S. Geological Survey Bulletin 1778, p. 37-59.

Blodgett, R.B., Clough, J.G., Harris, A.G., and Robinson, M. S., 1992, The Mount Copleston Limestone, a new Lower Devonian Formation in the Shublik Mountains, northeastern Brooks Range, Alaska, in Bradley, D.C., and Ford, A.B., eds., Geological studies in Alaska by the U.S. Geological Survey, U.S. Geological Survey Bulletin 1999, pp. 3-7.

Burbank, D., Meigs, A., and Brozovic, N., 1996, Interactions of growing folds and coeval depositional systems: Basin Research, v. 8, p. 199-223.

Clough, J.G., Robinson, M.S., Pessel, G.H., Imm, T.A., 1990, Geology and age of Franklinian and older rocks in the Sadlerochit and Shublik Mountains, Arctic National Wildlife Refuge, Alaska: Geological Association of Canada, Mineralogical Association of Canada Annual Meeting, 1990, Abstracts of Papers, v. 15, p. A25.

Carter, L. D., Ferrians, O.J., Jr., Galloway, J.P., 1986, Engineering-geologic maps of northern Alaska coastal plain and foothills of the Arctic National Wildlife Refuge: U. S. Geological Survey Open-File Report 86-0334.

Dumoulin, J.A., and Harris, A.G., 1994, Depositional framework and regional correlation of pre-Carboniferous metacarbonate rocks of the Snowden Mountain area, central Brooks Range, northern Alaska: U.S. Geological Survey Professional Paper 1545, 75 p.

Dutro, J.T., Jr., 1970, Pre-Carboniferous carbonate rocks, northeastern Alaska, in Adkinson, W.L., and Brosge, M.M., eds., Proceedings of the geological seminar on the North Slope of Alaska: Amer. Assoc. of Petrol. Geol., Pacific Section, p. M1-M8.

Fisher, M.A. and Bruns, T.R., 1987, Structure of pre-Mississippian rocks beneath the coastal plain, in Bird, K.J., and Magoon, L.B., eds., Petroleum Geology of the northern part of the Arctic National Wildlife Refuge, northeastern Alaska: U.S. Geological Survey Bulletin 1778, p. 245-248.

Gradstein, F.M., Agterberg, F.P., Ogg, J.G., Hardenbol, J., van Veen, P., Thierry, J., and Huang, Z., 1994, A Mesozoic time scale: Journal of Geophysical Research, v. 99, no. B12, p. 24,051-24,074.

Grantz, A., Holmes, M.L., and Kososki, B.A., 1975, Geologic framework of the Alaska continental terrace in the Chukchi and Beaufort Seas, in Yorath, Parker, and Glass, eds., Canada's continental margins and offshore petroleum exploration: Canadian Society of Petroleum Geologists Memoir 4, pp. 669-700.

Grantz, A., and May, S.D., 1983, Rifting history and structural development of the continental margin north of Alaska, in Watkins, J.S., and Drake, C.L., eds., Studies in Continental Margin Geology, AAPG Memoir 34, pp. 77-100.

Click here or on this symbol in the toolbar to return.

Grantz, A., Dinter, D.A., and Biswas, N.N., 1983, Map, cross sections, and chart showing late Quaternary faults, folds, and earthquake epicenters on the Alaskan Beaufort shelf: U.S. Geological Survey Miscellaneous Investigations Series, Map I-1182-C.

Grantz, A., Dinter, D.A., and Culotta, R.C., 1987, Structure of the continental shelf north of the Arctic National Wildlife Refuge in Bird, K.J., and Magoon, L.B., eds., Petroleum Geology of the northern part of the Arctic National Wildlife Refuge, northeastern Alaska: U.S. Geological Survey Bulletin 1778, pp. 271-276.

Hanks, C.L., Wallace, W.K., and O'Sullivan, P., 1994, The Cenozoic structural evolution of the northeastern Brooks Range, Alaska, in Thurston, D., and Fujita, K., eds., 1992 Proceedings International Conference on Arctic Margins, U.S. Minerals Management Service Outer Continental Shelf Study 94-0040, pp. 263-268.

Johnsson, M.J., Pawlewicz, J., Harris, A.G., and Valin, Z.C., 1992, Vitrinite reflectance and conodont color alteration index data from Alaska: U.S. Geological Survey Open-file Report 92-409, 3 computer disks, 1 sheet.

Kelley, J. S., and Foland, R.L., 1987, Structural style and framework geology of the coastal plain and adjacent Brooks Range, in Bird, K.J., and Magoon, L.B., eds., Petroleum Geology of the northern part of the Arctic National Wildlife Refuge, northeastern Alaska: U.S. Geological Survey Bulletin 1778, p. 255-270.

Kelley, J.S., and Molenaar, C.M., 1987, Detachment tectonics in the Sadlerochit and Shublik Mountains and applications for exploration beneath the coastal plain, Arctic National Wildlife Refuge, Alaska, in Tailleur, I., and Weimer, P., eds., Alaskan North Slope Geology, Pacific Section, Society of Economic Paleontologists and Mineralogists, Bakersfield, California, abstract, p757.

Knock, D.G., 1986, Thirty-seven measured sections of Lower Cretaceous Kemik Sandstone, northeastern Alaska: Alaska Divisions of Mining and Geological and Geophysical Surveys Public Data File 86-86b, 21 p., 7 sheets.

Click here or on this symbol in the toolbar to return.

Knock, D.G., 1987, Lithofacies, depositional setting, and petrography of the Kemik Sandstone, Arctic National Wildlife Refuge (ANWR), northeastern Alaska: Master of Science thesis, University of Alaska, Fairbanks, 135 p.

Leiggi, P.A., 1987, Style and age of tectonism of the Sadlerochit Mountains to Franklin Mountains, Arctic National Wildlife Refuge, Alaska, in Tailleur, I., and Weimer, P., eds., Alaskan North Slope Geology, Pacific Section, Society of Economic Paleontologists and Mineralogists, Bakersfield, California, pp. 749-756.

Lerand, M., 1973, Beaufort Sea, in McCrossam, R.G., ed., The future petroleum provinces of Canada-- Their geology and potential: Canadian Society of Petroleum Geology Memoir 1, pp. 315-386.

Meigs, A.J., 1989, Structural geometry and sequence in the eastern Sadlerochit Mountains, northeastern Brooks Range, Alaska: Master of Science thesis, University of Alaska, Fairbanks, Alaska, 220 p.

Molenaar, C.M., Bird, K.J., and Collett, T.S., 1986, Regional correlation sections across the North Slope of Alaska, U.S. Geological Survey, Miscellaneous Field Studies, Map MF-1907.

Moore, T.E., Wallace, W.K., Bird, K.J., Karl, S.M., Mull, C.G., and Dillon, J.T., 1994, Geology of northern Alaska, in Plafker, G., and Berg, H.C., eds., The Geology of Alaska: Boulder, Colorado, Geological Society of America, The Geology of North America, v. G-1, pp. 49-140.

Mull, C.G., 1987, Kemik Sandstone, Arctic National Wildlife Refuge, northeastern Alaska, in Tailleur, I., and Weimer, P., eds., Alaskan North Slope Geology, Field Trip Guidebook: Pacific Section, Society of Economic Paleontologists and Mineralogists, Bakersfield, California, pp. 405-431.

Mull, C.G., and Decker, J., 1993, Organic-rich shale and bentonite in the Arctic Creek unit, Arctic National Wildlife Refuge: Implications for stratigrapic and structural interpretations, in Solie, D., and Tannian, F., eds., Short Notes on Alaskan Geology, 1993: State of Alaska Division of Geological and Geophysical Surveys, Professional Report 113, pp. 41-50.

Click here or on this symbol in the toolbar to return.

Mull, C.G., and Anderson, A.V., 1991, Franklinian lithotectonic domains, northeastern Brooks Range, Alaska, Alaska Division of Geological and Geophysical Surveys, Public-data File 91-5, 40 p.

Oldow, J.S., Avé Lallemant, H.G., and Julian, F.E., and Seidensticker, C.M., 1987, Ellesmerian(?) and Brookian deformation in the Franklin Mountains, northeastern Brooks Range, Alaska, and its bearing on the origin of the Canada basin: Geology, v. 15, p. 37-41.

O'Sullivan, P.B., 1993, Late Mesozoic to Cenozoic thermal and uplift history of the North Slope foreland basin, northern Alaska and northwestern Canada, La Trobe University, Bundoora, Australia, Ph.D thesis, 419 p.

O'Sullivan, P.B., 1994, Timing of Tertiary episodes of cooling in response to uplift and erosion, northeastern Brooks Range, Alaska, in Thurston, D.K., and Fujita, K., eds., 1992 Proceedings International Conference on Arctic Margins: Anchorage, Alaska, Minerals Management Service OCS Study MMS 94-0040, p. 269-274.

O'Sullivan, P.B., Green, P.F., Bergman, S.C., Decker, J., Duddy, I.R., Gleadow, A.J.W., and Turner, D.L., 1993, Multiple phases of Tertiary uplift and erosion in the Arctic National Wildlife Refuge, Alaska, revealed by apatite fission-track analysis: American Association of Petroleum Geologists Bulletin, v. 77, pp. 359-385.

O'Sullivan, P.B., Wallace, W.K., Green, and Murphy, J., In prep., Middle Eocene and late Oligocene compression within the Sadlerochit Mountains region of the northeastern Brooks Range, Alaska: Implications for hydrocarbon accumulation in the Arctic National Wildlife Refuge.

Rattey, R.P., 1987, Northeastern Brooks Range, Alaska: New evidence for complex thin-skinned thrusting, in Tailleur, I., and Weimer, P., eds., Alaskan North Slope Geology, Pacific Section, Society of Economic Paleontologists and Mineralogists, Bakersfield, California, abstract, pp. 757.

Reed, B.L., 1968, Geology of the Lake Peters area, northeastern Brooks Range, Alaska: U.S. Geological Survey Bulletin 1236, 132 p.

Rejebian, V.A., Harris, A.G., and Huebner, J.S., 1987, Conodont color and textural alteration: An index to regional metamorphism, contact

metamorphism, and hydrothermal alteration: GSA Bulletin, v. 99, p. 471-479.

Reiser, H.N., Brosg_, W.P., Dutro, J.T., Jr., and Detterman, R.L., 1971, Preliminary geologic map, Mt. Michelson Quadrangle, Alaska, U. S. Geological Survey, Open File Report 71-0237.

Reiser, H.N., Brosg_, W.P., Dutro, J.T., and Detterman, R.L., 1980, Geologic map of the Demarcation Point quadrangle, Alaska: U.S. Geological Survey Miscellaneous Investigations Series Map I-1133, scale 1:250,000.

Robinson, M.S., Decker, J., Clough, J.G., Reifenstuhl, R.R., Dillon, J.T., Combellick, R.A., and Rawlinson, S.E., 1989, Geology of the Sadlerochit and Shublik Mountains Arctic National Wildlife Refuge, northeastern Alaska: Professional Report 100, Alaska Department of Natural Resources, Division of Geological and Geophysical Surveys. 1 sheet, scale 1:63,360.

Rogers, J.A., 1989, Structural evolution of the central Shublik Mountains and Ignek Valley, northeastern Brooks Range, Alaska: Alaska Division of Geological and Geophysical Surveys Public Data-File 89-1c, 36 p.

Rogers, J.A., 1992, Lateral variation of range-front structures and structural evolution of the central Shublik Mountains and Ignek Valley, northeastern Brooks Range, Alaska: Master of Science thesis, University of Alaska, Fairbanks, 128 p.

Rowan, E.L., 1997, Basin evolution, and the timing and extent of oil generation, Canning River region, North Slope, Alaska: Preliminary Basin2 calculations assuming a conductive thermal history: U.S. Geological Survey, Open File Report 97-711.

Sassi, W., and Rudkiewicz, J.L., 1996, Thrustpack version 3.3: 2D integrated maturity studies in thrust areas, Institut Français du Pétrole, Report 43393, 122 p.

Suppe, J., 1983, Geometry and kinematics of fault-bend folding: American Journal of Science, v. 283, pp. 684-721.

Click here or on this symbol in the toolbar to return.

Suppe, J., 1985, Principles of structural geology: Prentice-Hall, Englewood Cliffs, New Jersey, 537 p.

Wallace, W.K., 1993, Detachment folds and a passive-roof duplex: Examples from the northeastern Brooks Range, Alaska in Solie, D.N., and Tannian, F., eds., Short Notes on Alaskan geology 1993: Alaska Division of Geological and Geophysical Surveys Professional Report 113, p. 81-99.

Wallace, W.K., and Hanks, C.L., 1990, Structural provinces of the northeastern Brooks Range, Arctic National Wildlife Refuge, Alaska: American Association of Petroleum Geologists Bulletin, v. 74, p. 1100-1118.

Wallace, W.K., Moore, T.E., and Plafker, G., 1997, Multistory duplexes with forward dipping roofs, north central Brooks Range, Alaska: Journal of Geophysical Research, v. 102, no. B9, p. 20,773-20,796.

Click here or on this symbol in the toolbar to return.

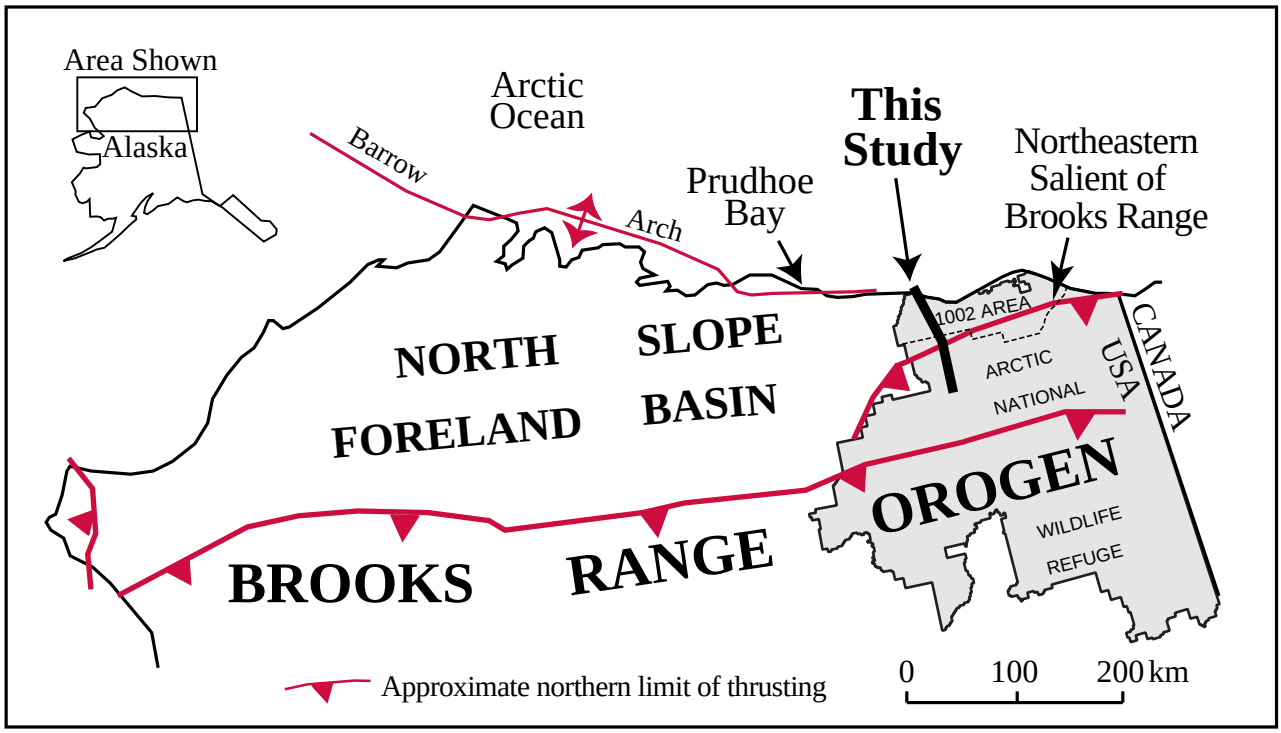

Figure SM1. Index map of northern Alaska, showing Brooks Range orogen, North Slope foreland basin, northeastern salient of Brooks Range, Arctic National Wildlife Refuge, 1002 Area, and location of this study.

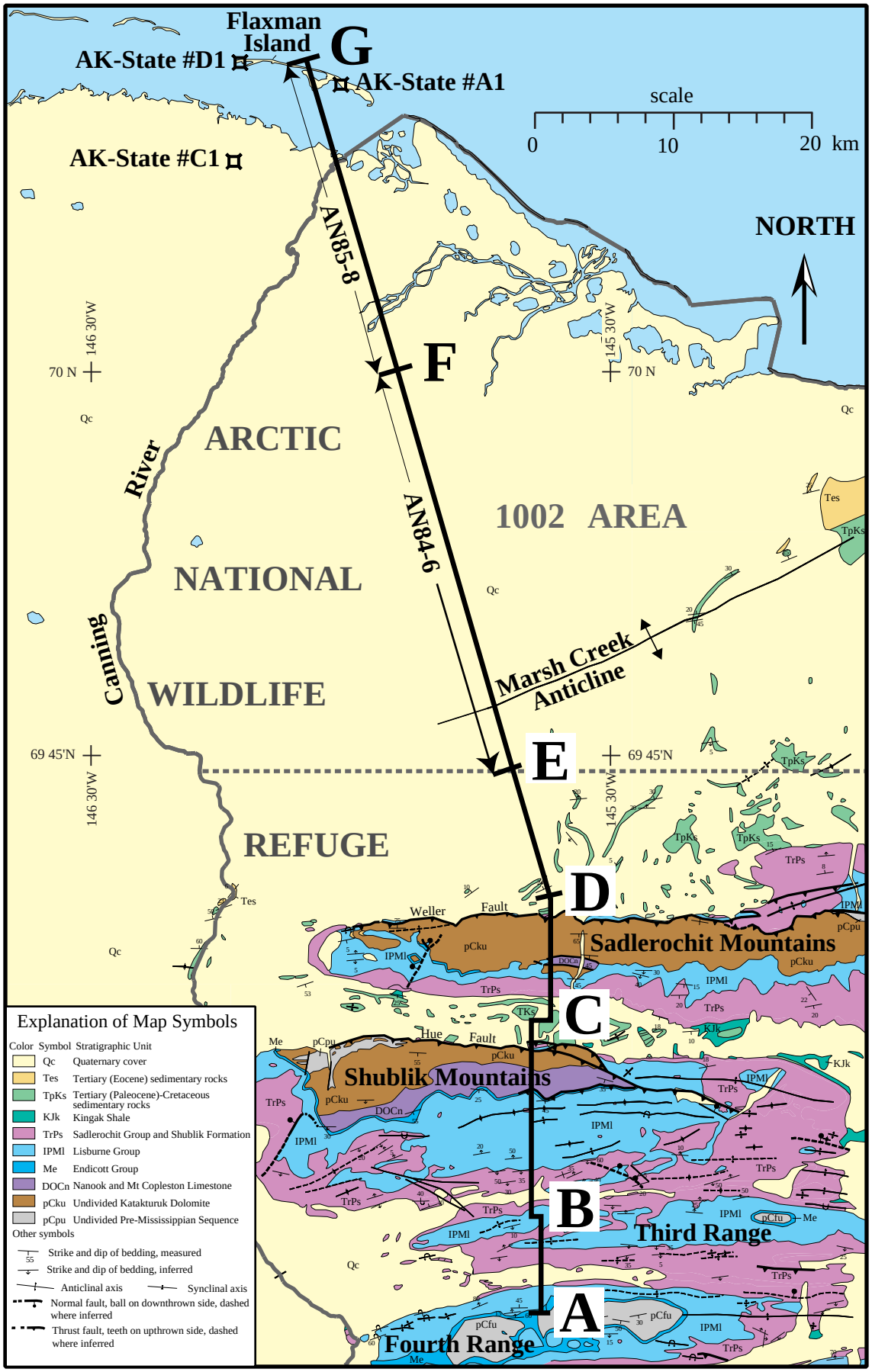

Figure SM2. Geologic map of western Arctic National Wildlife Refuge, Alaska, showing location of this transect, A-G.

Click here or on this symbol
in the toolbar to return.

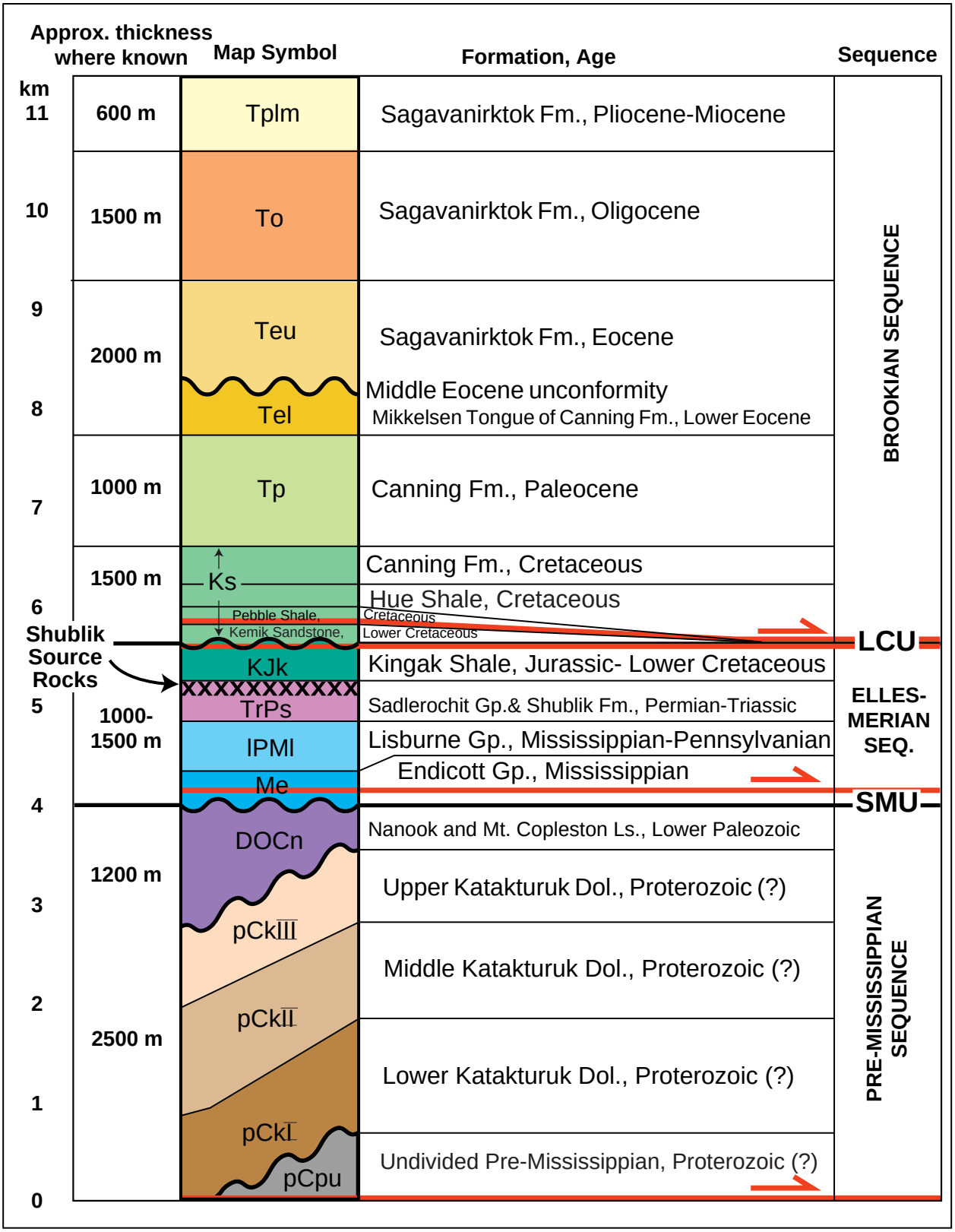

Figure SM3. Generalized composite stratigraphy along transect A-G (location shown in figure SM2), in western Arctic National Wildlife Refuge, Alaska; see plate SM1, for explanation of map symbols.

Click here or on this symbol
in the toolbar to return.

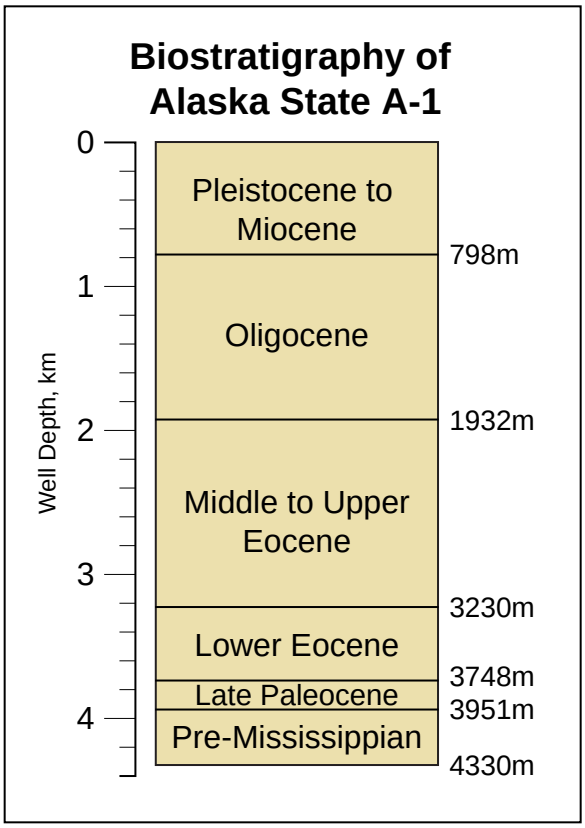

Figure SM4. Biostratigraphy for the Alaska State A-1 well, based on W. Poag, Chap. BI.

Click here or on this symbol
in the toolbar to return.

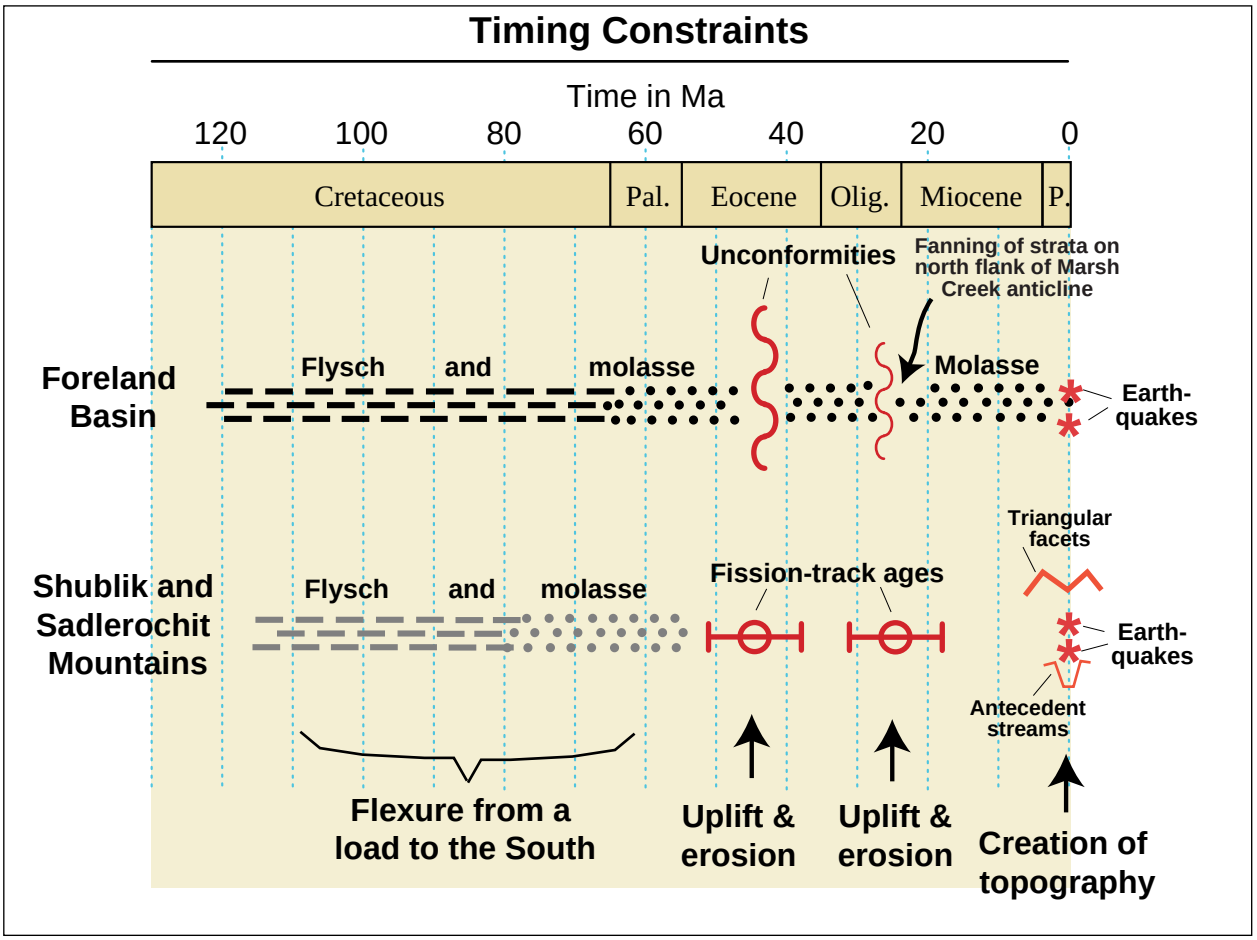

Figure SM5. Constraints used to deduce timing of deformation along transect A-G.

Click here or on this symbol
in the toolbar to return.

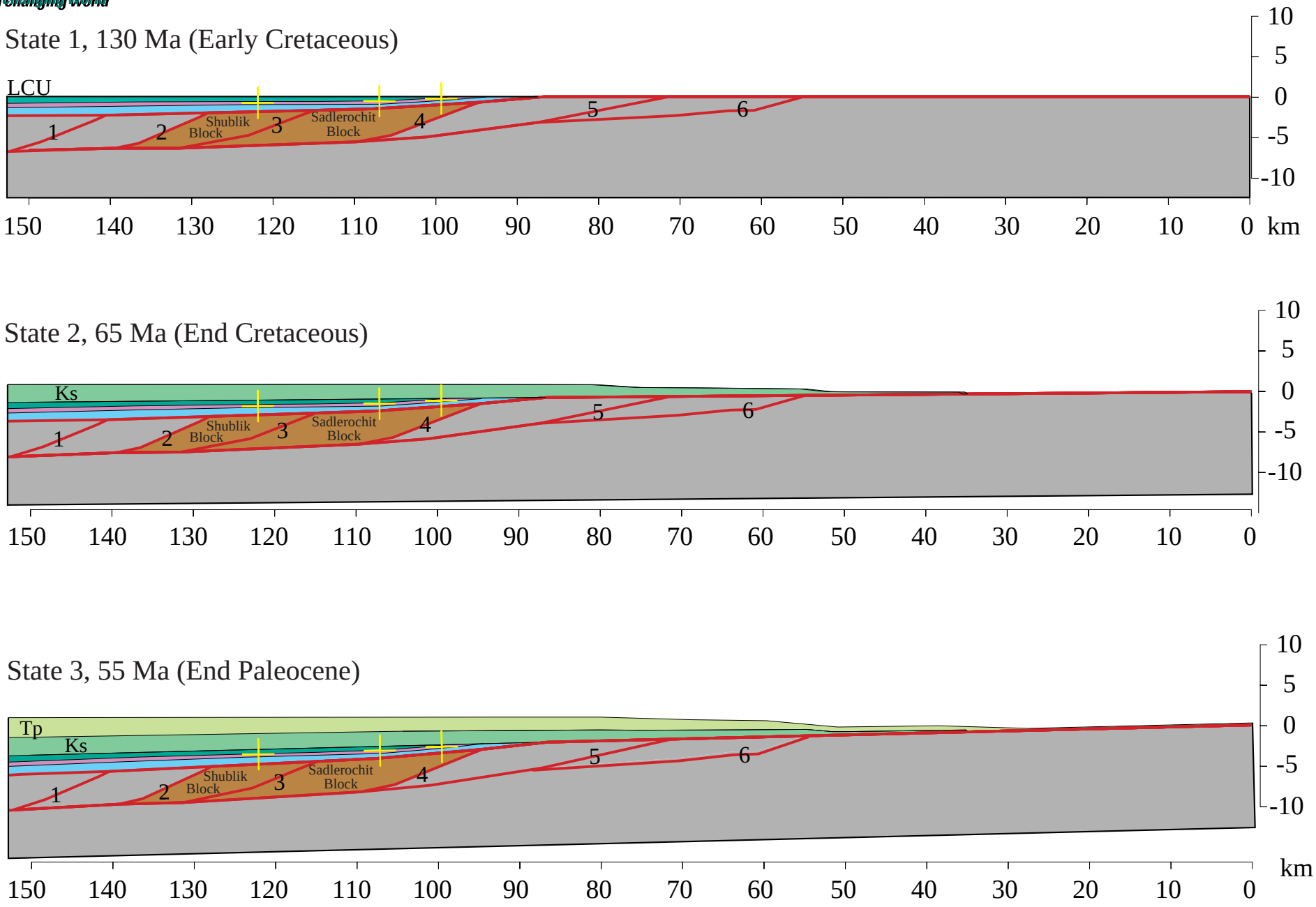

Figure SM6A. Forward model (Part A) created with Thrustpack to show major sedimentation and deformation events along transect A-G (location shown in figure SM2 and plate SM1); see table SM1 for model input.

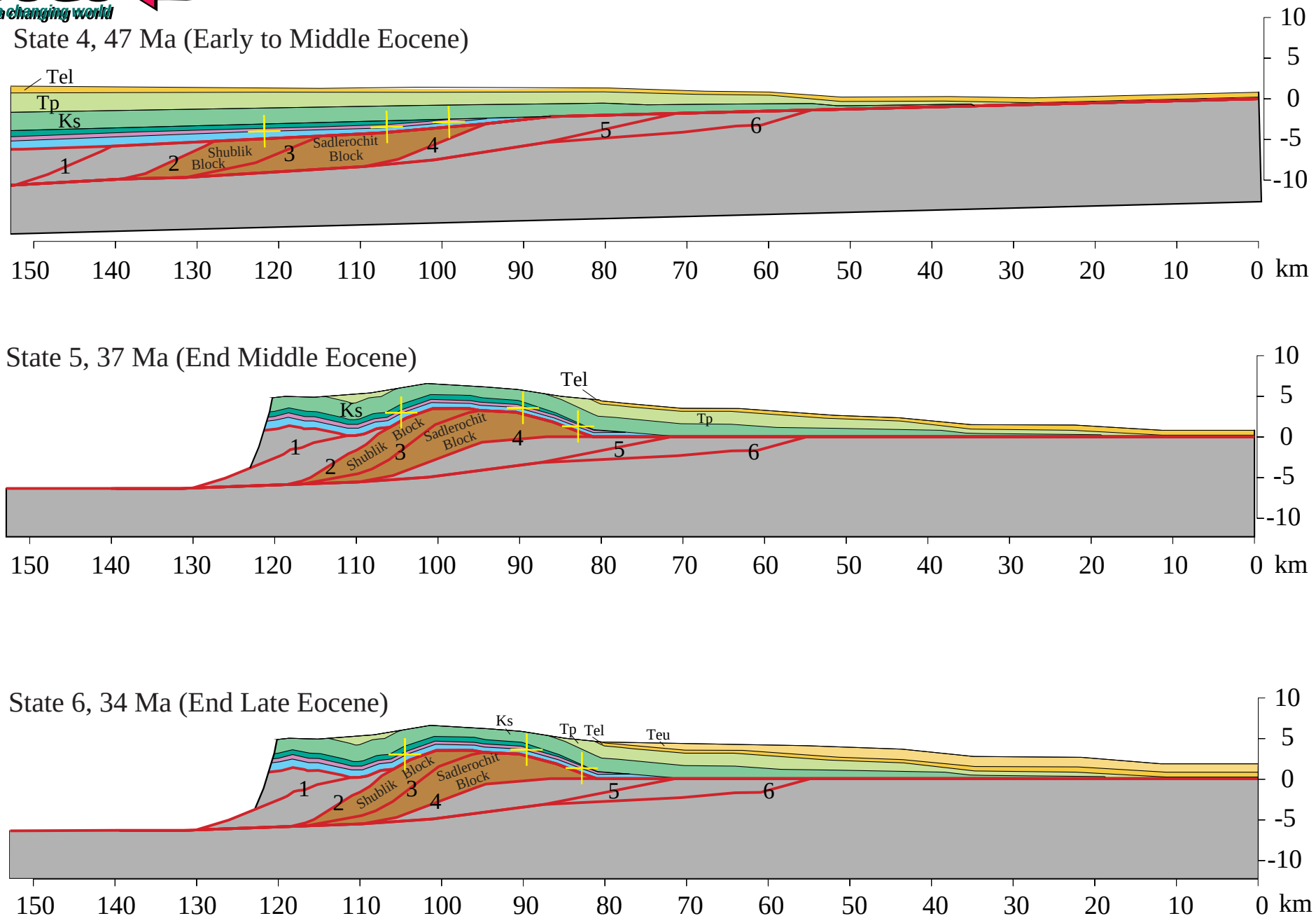

Figure SM6B. Forward model (Part B) created with Thrustpack to show major sedimentation and deformation events along transect A-G (location shown in figure SM2 and plate SM1); see table SM1 for model input.

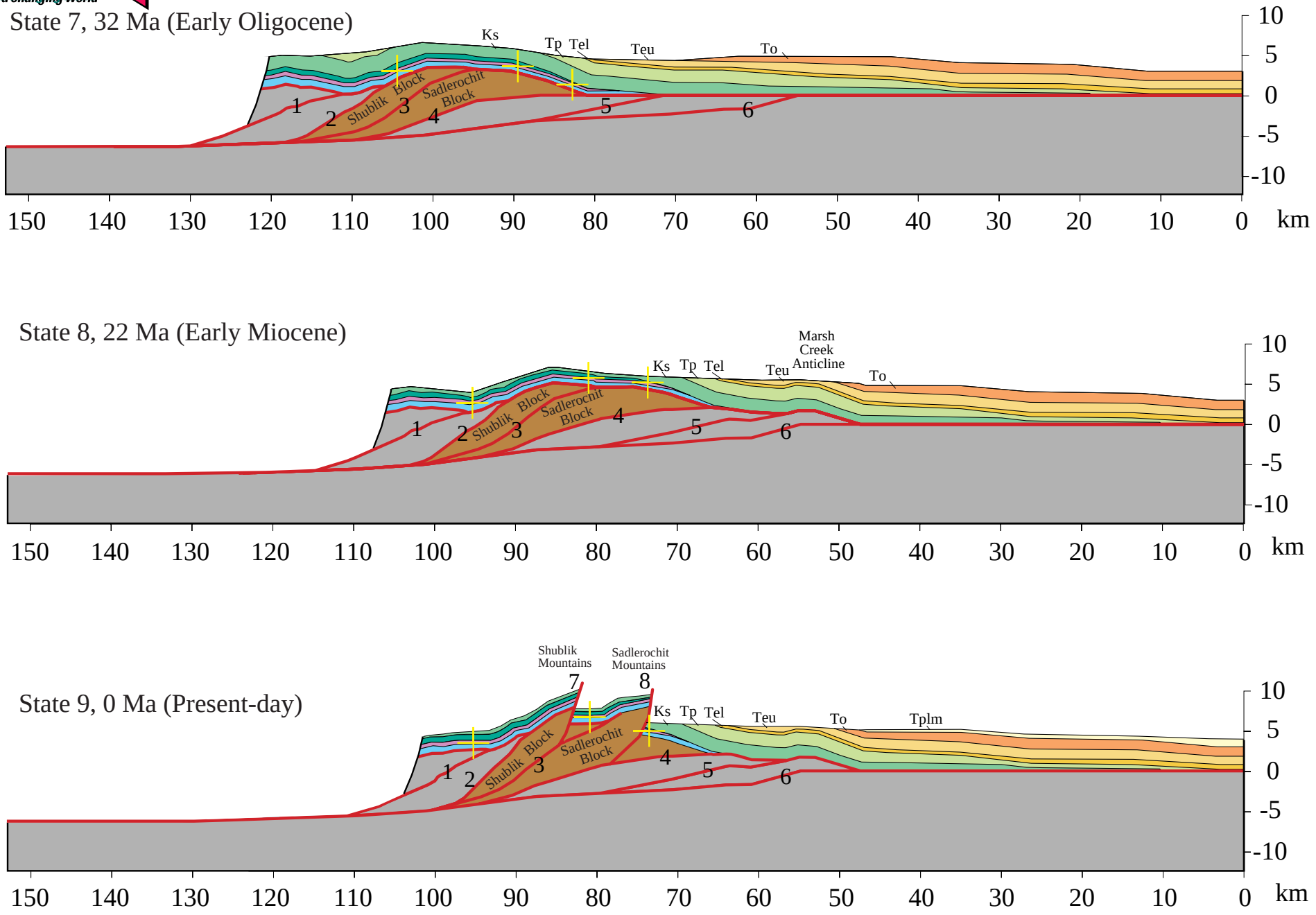

Figure SM6C. Forward model (Part C) created with Thrustpack to show major sedimentation and deformation events along transect A-G (location shown in figure SM2 and plate SM1); see table SM1 for model input.

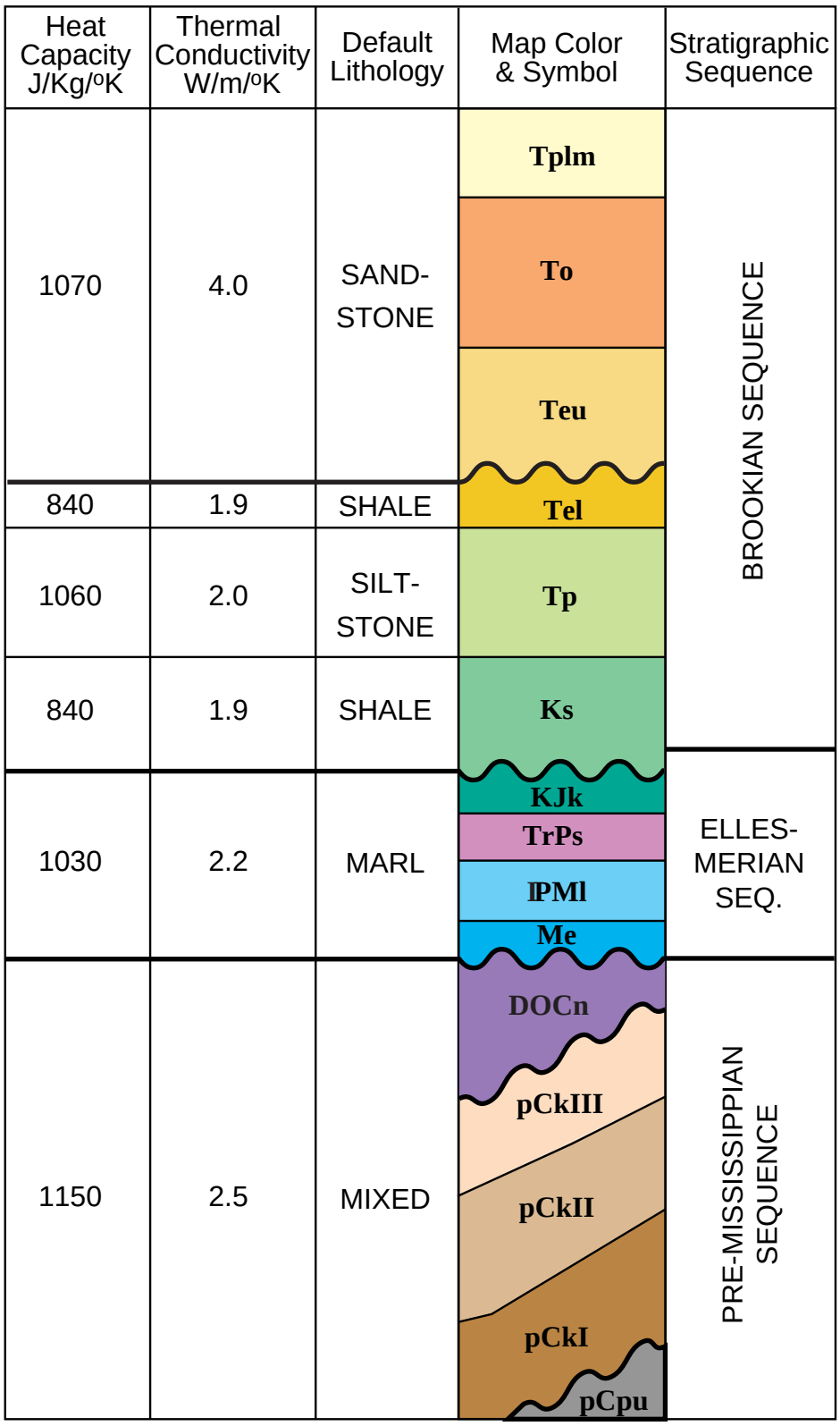

Figure SM7. Thermal properties and default lithologies used for thermal modeling with Thrustpack.

Click here or on this symbol
in the toolbar to return.

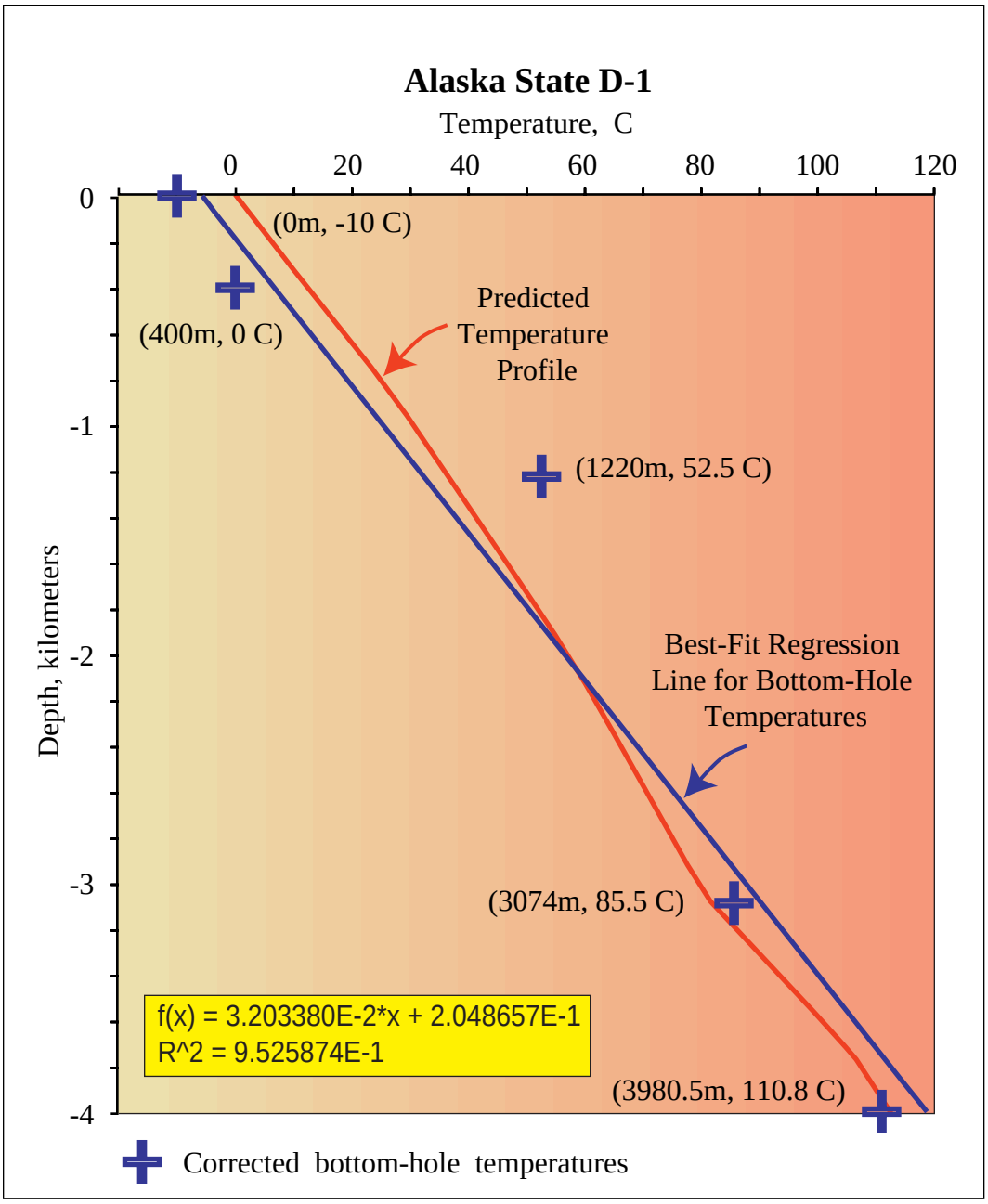

Figure SM8. Comparison of observed and predicted temperatures at the Alaska State D-1 well (location shown in figure SM2 and Plate SM1); blue profile based on corrected bottom-hole temperatures from the Alaska State D-1 well; red profile based on Thrustpack model, using thermal conductivities shown in figure SM5, and a basal heat flow of 55 mW/m2 at 20 km depth.

Click here or on this symbol
in the toolbar to return.

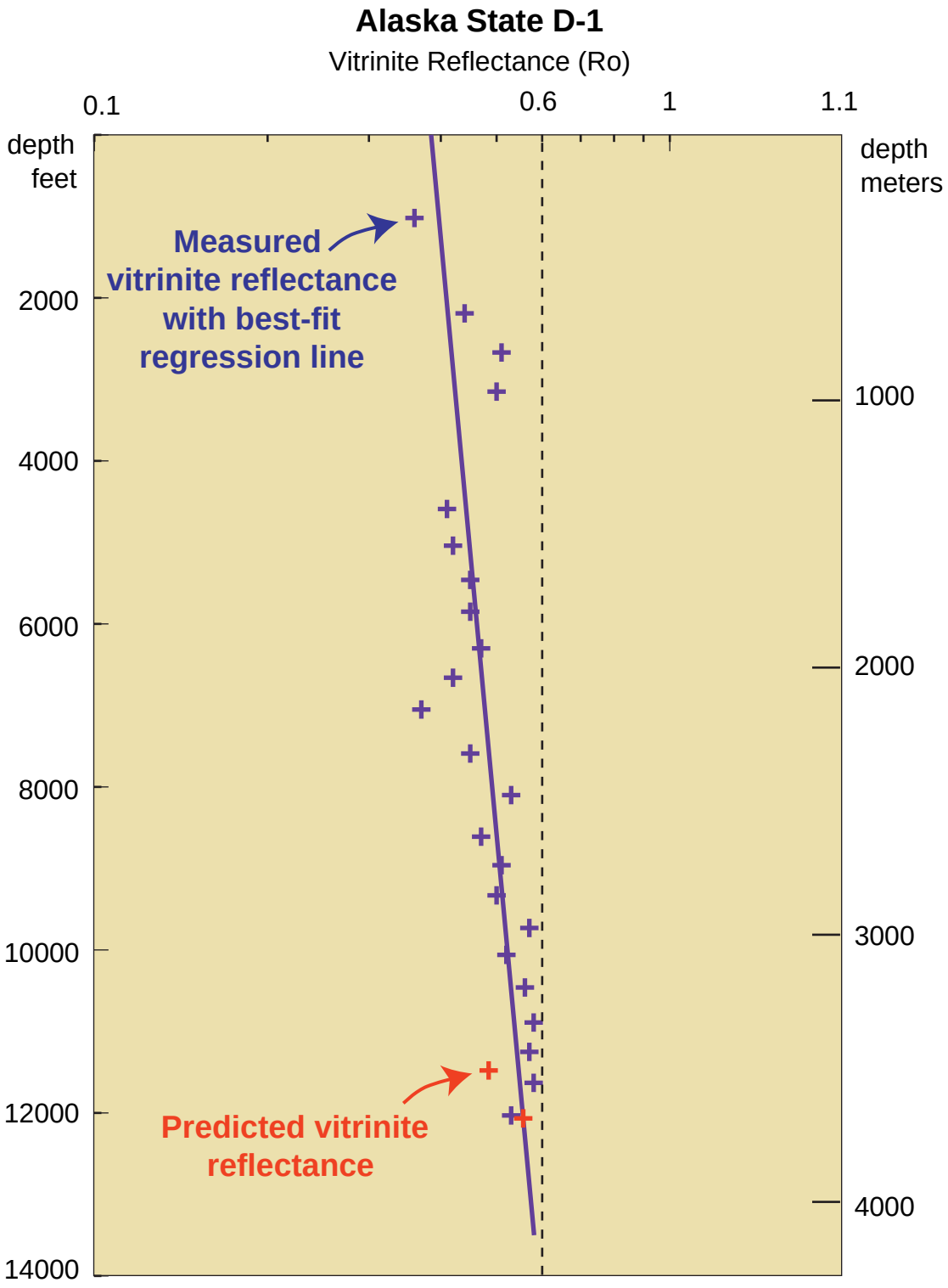

Figure SM9. Comparison of observed and predicted vitrinite reflectance at the Alaska State D-1 well; blue symbols, measured values; red symbols, predicted values based on our Thrustpack model. Thermal conductivities as in figure SM5, basal heat flow 55mW/m2 at 20 km depth.

Click here or on this symbol
in the toolbar to return.

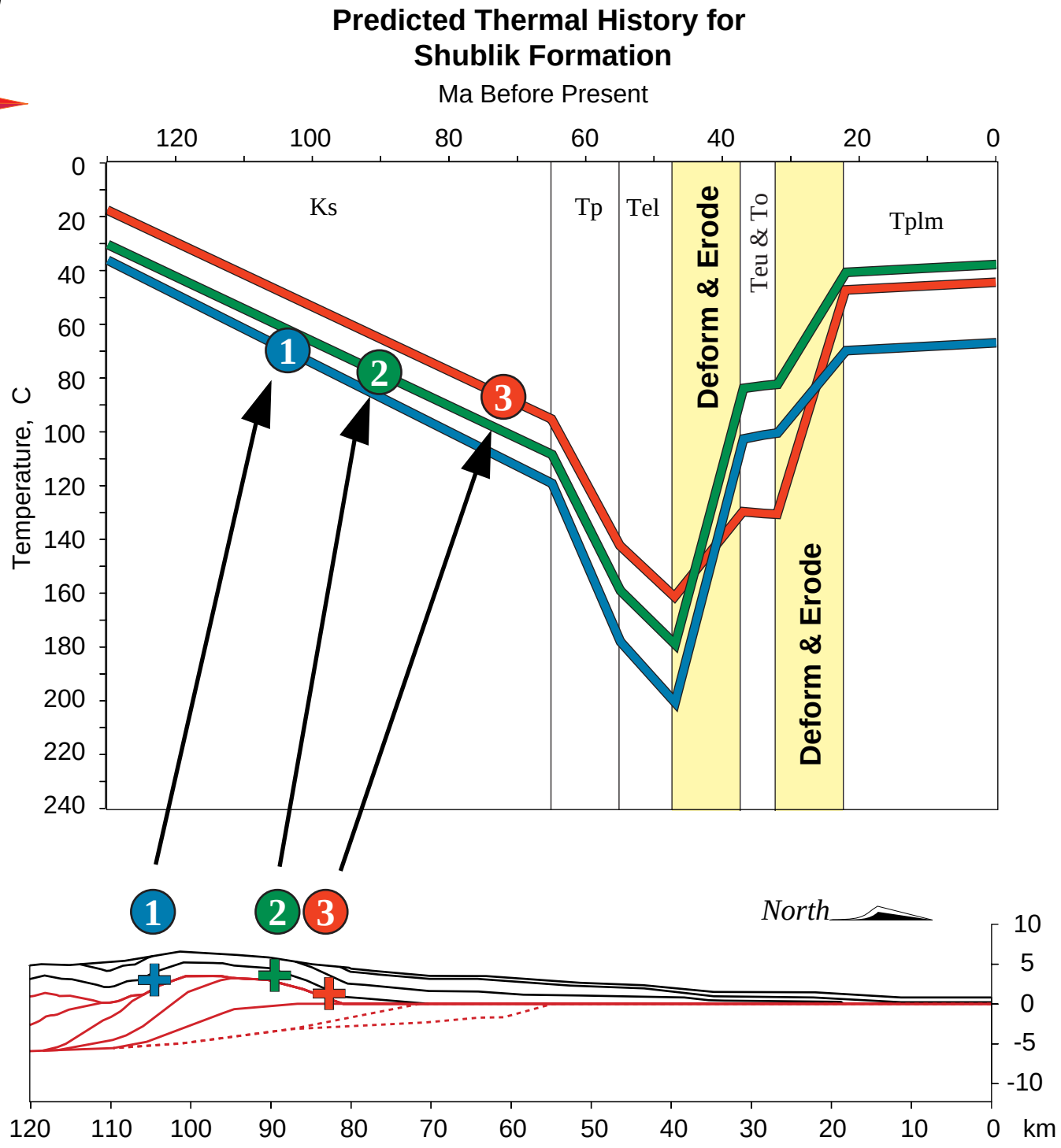

Figure SM10. Predicted temperature histories for three history points in the Shublik Formation. Stratigraphic labels correspond to those in plate SM1.

Click here or on this symbol
in the toolbar to return.

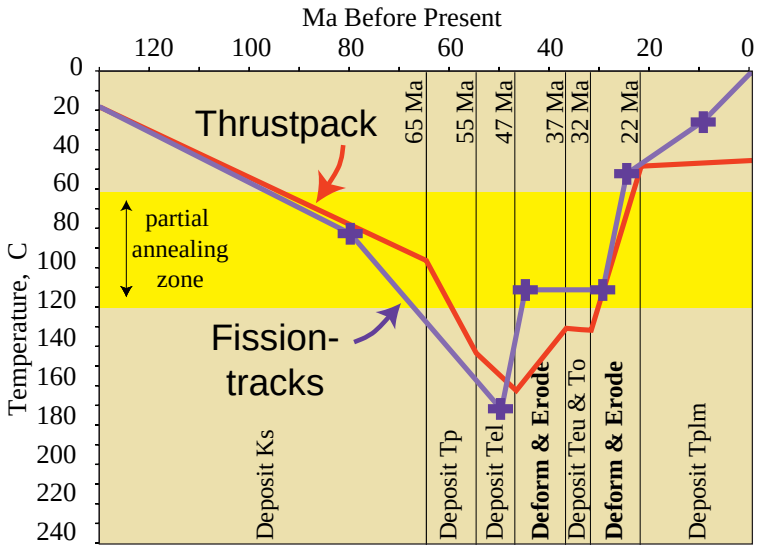

Figure SM11. Comparison of modeled thermal histories at Sadlerochit Mountain front. Blue symbols and blue line, thermal history derived from apatite fission-track ages in Triassic rocks at Sadlerochit Mountain front (sample 91POS77 in O'Sullivan et al., in prep); red line, predicted thermal history for Shublik Formation at same location based on Thrustpack modeling.

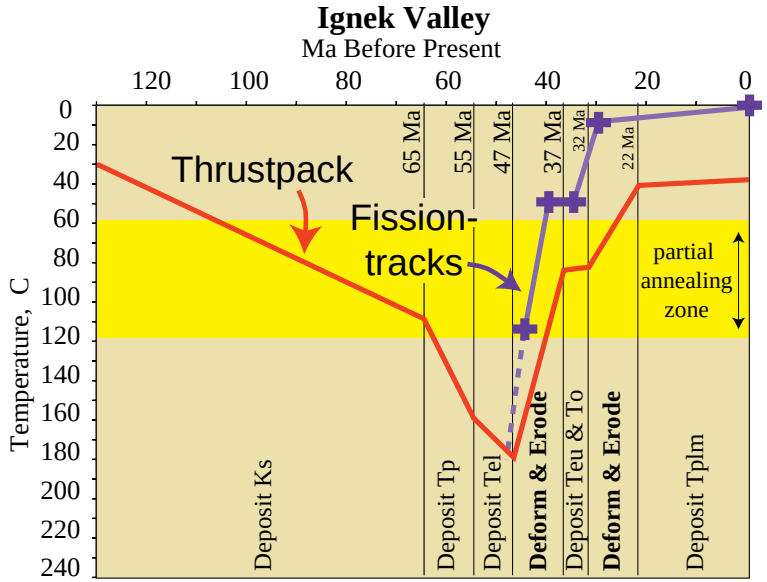

Figure SM12. Comparison of modeled thermal histories at Ignek Valley. Blue symbols and blue line, thermal history modeled from apatite fission-track ages in Cretaceous rocks at Ignek Valley (O'Sullivan, 1993; O'Sullivan, 1994); red line, predicted thermal history for the Shublik Formation at the same location, based on Thrustpack modeling.

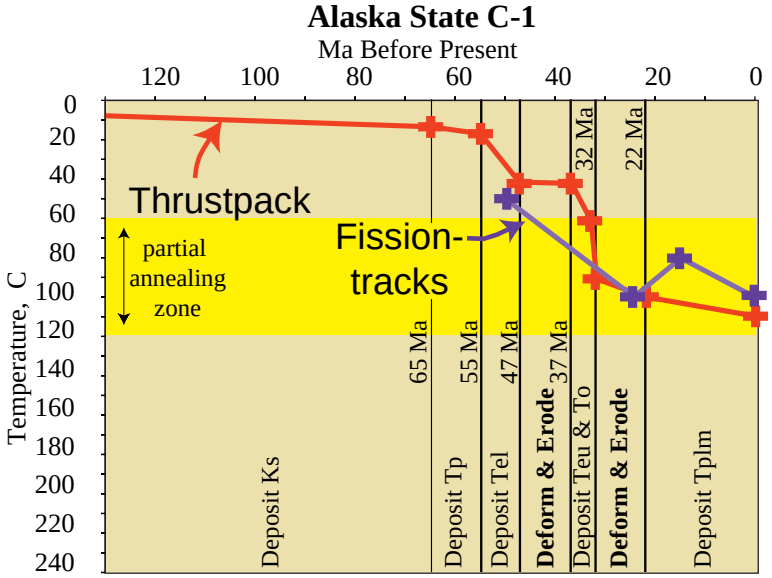

Figure SM13. Comparison of modeled thermal histories at Alaska State C-1 well. Blue symbols and blue line, thermal history modeled from apatite fission-track ages in Cretaceous rocks at the base of the Brookian sequence (O'Sullivan, 1993); red line, predicted thermal history for the basal Brookian sequence at the same location, based on Thrustpack modeling.

Click here or on this symbol in the toolbar to return.

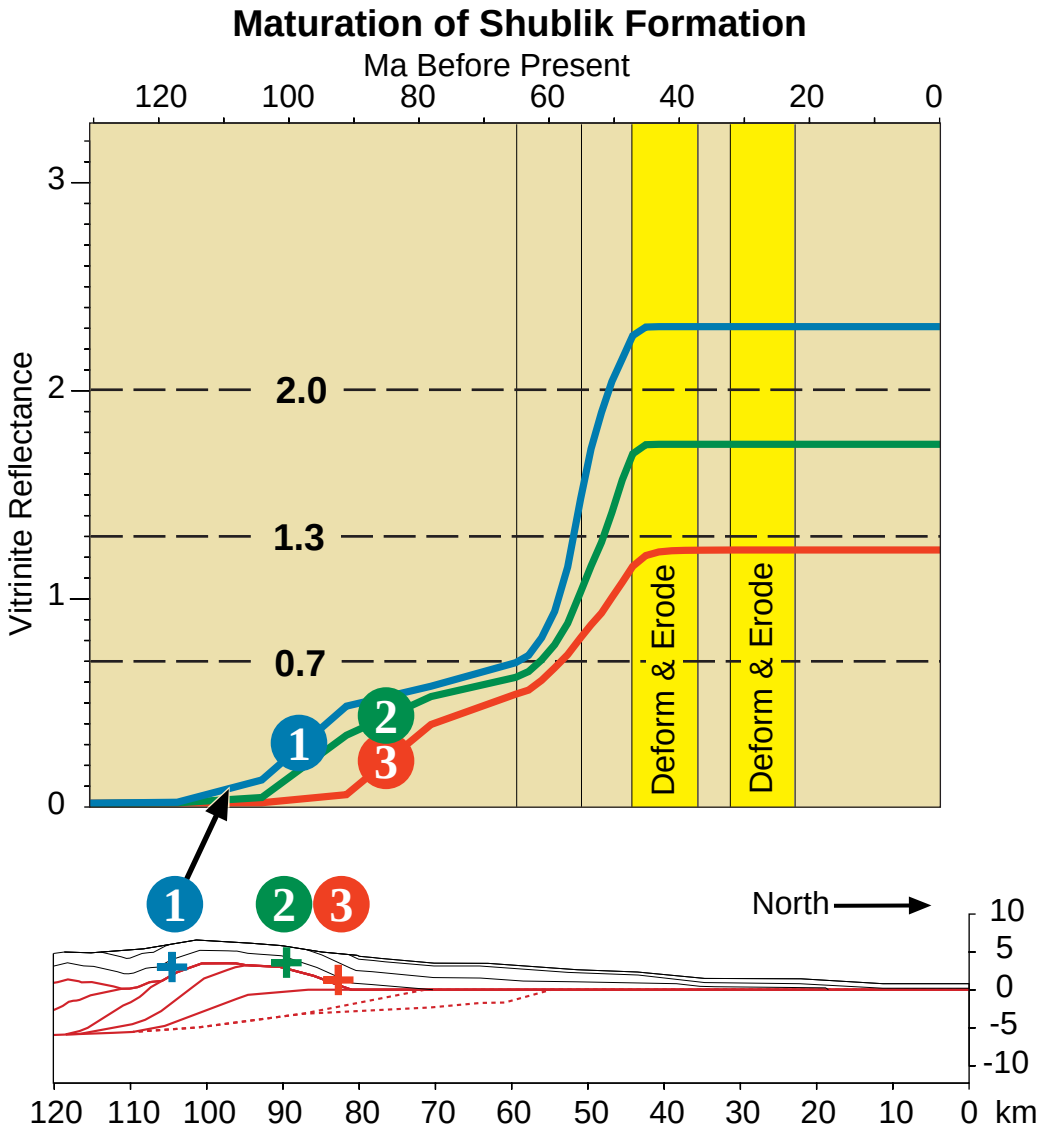

Figure SM14. Predicted maturation history for three history points in the Shublik Formation, according to our Thrustpack model.

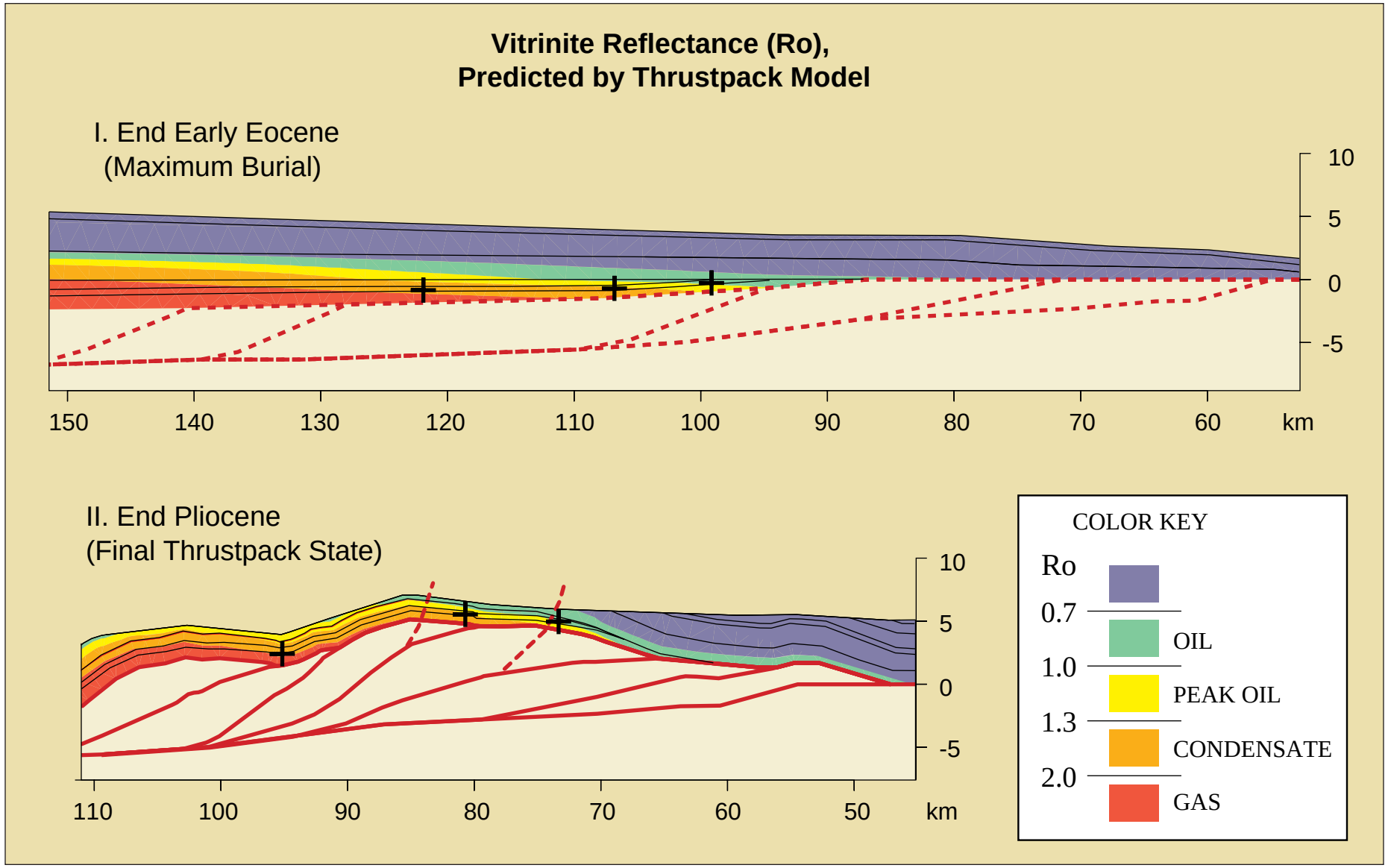

Figure SM15. Colored zones of vitrinite reflectance (Ro), as calculated by Thrustpack, for rocks of Ellesmerian and Brookian sequences; I, End Early Eocene (time of maximum burial); II, End Pliocene (final Thrustpack state for thermal calculations).

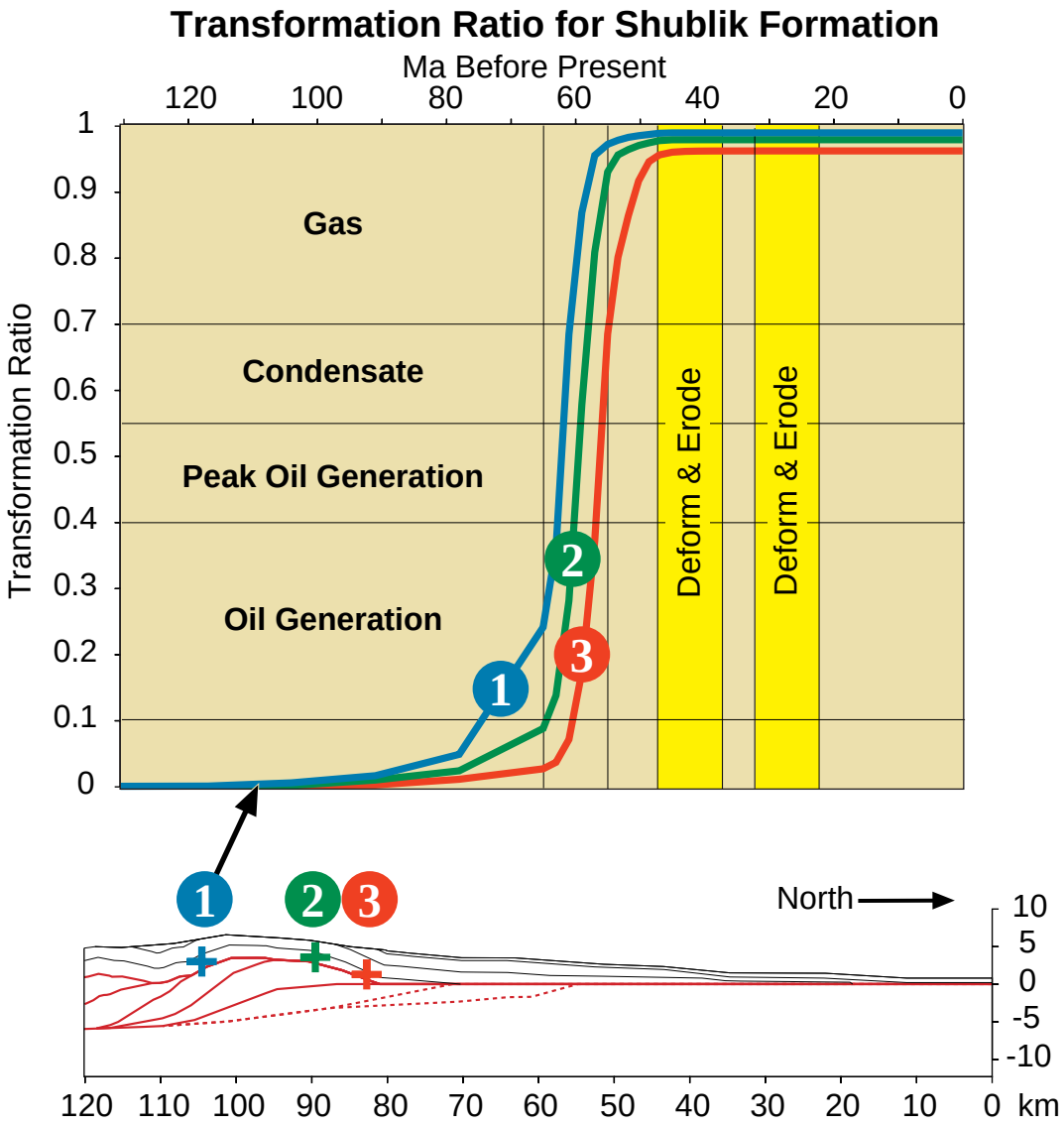

Figure SM16. Predicted evolution of transformation ratio for three history points in the Shublik Formation, according to our Thrustpack model.

U.S.DEPARTMENT OF INTERIOR
U.S. GEOLOGICAL SURVEY

OPEN-FILE REPORT 98-34
PLATE SM1

A. Balanced Cross Section

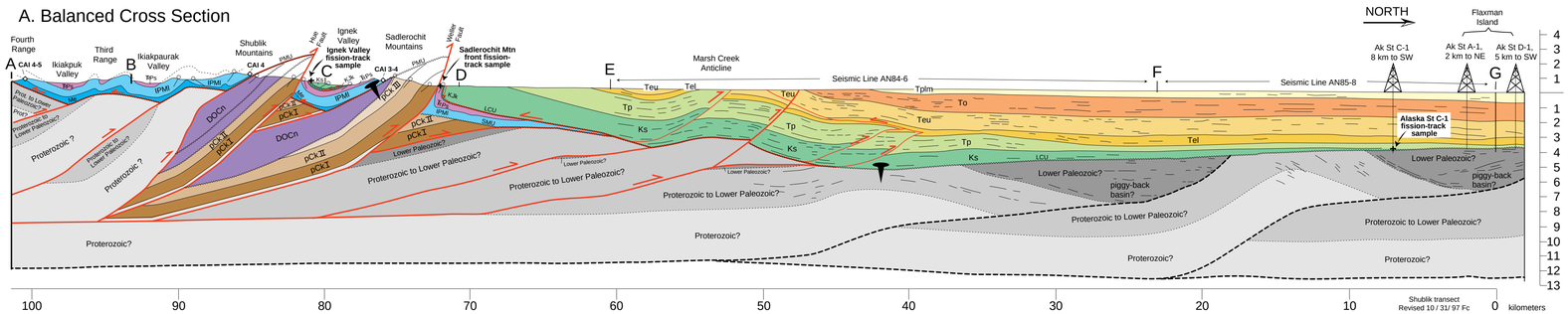

B. Structural-Stratigraphic Restoration of Cross Section

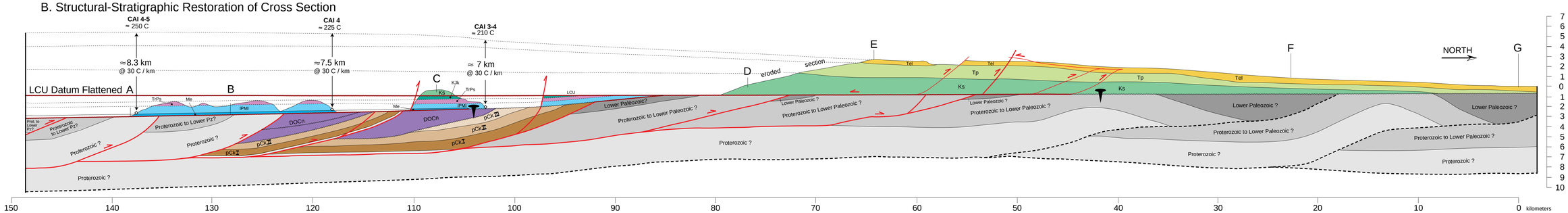

Explanation

Brookian Sequence (except Kemik Sandstone and pebble shale unit of Ks)

- Tplm — Miocene-Pliocene sedimentary rocks, mainly Sagavanirktok Formation at Flaxman Island [1]
- To — Oligocene sedimentary rocks, mainly Sagavanirktok Formation at Flaxman Island [1]
- Teu — Upper Eocene sedimentary rocks, mainly Canning Formation at Flaxman Island [1]
- Middle Eocene unconformity
- Tel — Lower Eocene sedimentary rocks, mainly Canning Formation at Flaxman Island [1]
- Tp — Paleocene sedimentary rocks, mainly Canning Formation at Flaxman Island [1]
- Ks — Cretaceous sedimentary rocks, includes Kemik Sandstone, pebble shale unit, Hue Shale, and lower part of Canning Formation [2]

Ellesmerian Sequence

- LCU — Lower Cretaceous unconformity
- KJk — Jurassic to Lower Cretaceous shale (Kingak Shale) [2]
- TrPs — Permian to Upper Triassic sedimentary rocks (Sadlerochit Group and Shublik Formation) [2]
- IPMI — Mississippian to Lower Pennsylvanian carbonate rocks (Lisburne group) [2]
- Me — Lower Mississippian shale and conglomerate (Endicott group) [2]

Pre-Mississippian Sequence

- SMU — sub-Mississippian unconformity
- DOCn — Cambrian to Devonian carbonate rocks (Nanook and Mount Copleston Limestone) [2]
- Unnamed unconformity
- pCk III — Proterozoic (?) dolomite (Katakturuk Dolomite, upper part), includes pEkbk, pEkh, pEkb, pEkus of Robinson et al. [2]
- pCk II — Proterozoic (?) dolomite (Katakturuk Dolomite, middle part), includes pEkw, pEkbn, pEklc, pEka, pEkuc, pEkp of Robinson et al. [2]
- pCk I — Proterozoic (?) dolomite and greenstone (Katakturuk Dolomite, lower part) includes pEkgn, pEks, pEkz, pEkv, pEkc, pEkl, pEkso of Robinson et al. [2]

Katakturuk Dolomite

Inferred basement units

- Lower Paleozoic? — *Inferred* Lower Paleozoic rocks (possibly including age-equivalents of the Nanook and Mount Copleston Limestones)
- Proterozoic to Lower Paleozoic? — *Inferred* Proterozoic to Lower Paleozoic rocks (possibly including age-equivalents of the Katakturuk Dolomite and Nanook and Mount Copleston Limestones)
- Proterozoic? — *Inferred* Proterozoic rocks (possibly including units that underlie the Katakturuk Dolomite)

Contacts and Symbols

- Brookian age fault, basement not involved
- Brookian age fault, basement involved
- Inferred pre-Mississippian age fault in basement
- Unconformity
- Stratigraphic contact
- Seismic Reflections
- G — Geographic location tied to accompanying geologic map
- Pin indicating unfaulted, depositional contact
- Bedding attitude
- CAI 3-4 — Approximate location of Conodont sample, showing conodont alteration index (CAI)
- Ignek Valley fission-track sample — Apatite Fission-Track Sample Location

[1] Molenaar, C.M., Bird, K.J., and Collett, T.S., 1986, Regional correlation sections across the North Slope of Alaska, U.S. Geological Survey Miscellaneous Field Studies, Map MF-1907, 1 sheet
[2] Robinson, M.S., Decker, J., Clough, J.G., Reifenstuhl, R.R.,Bakke, A., Dillon, J.T., Combellick, R.A., and Rawlinson, SE., 1989, Geology of the Sadlerochit and Shublik Mountains, Arctic National Wildlife Refuge, northeastern Alaska, Alaska Division of Geological and Geophysical Surveys, Professional Report 100

BALANCED CROSS SECTION AND STRUCTURAL STRATIGRAPHIC RESTORATION OF TRANSECT A-G (LOCATION SHOWN IN FIGURE SM2), IN THE WESTERN PART OF THE ARCTIC NATIONAL WILDLIFE REFUGE, ALASKA

By
Frances Cole, Kenneth J. Bird, Charles G. Mull, Wesley K. Wallace, William Sassi, John M. Murphy, and Myung Lee

1998

Table SM1. Input parameters for Thrustpack used to generate kinematic models shown in Figure 6. Fault numbers 1-8, correspond to those in Figure 6. Units Ks, Tp, Tel, Teu, To, and Tplm correspond to those shown in Plate 1. Surface temperatures used for thermal computations (far right column) are generalized from Rowan, 1997. Absolute time in Ma according to the timescales of Gradstein and others (1994) and Berggren and others (1995).

State No.	**Time, Ma.**	**Fault Number with Fault Displacement in km**								**Model-Simulated Events (Deposition, Deformation, and/or Erosion)**	**Surface Temperature, ^{o}C**
		1	**2**	**3**	**4**	**5**	**6**	**7**	**8**		
1	130									End of passive margin; erosion on L. Cretaceous unconformity.	9
2	130-65									Deposit Ks (Kemik Sandstone, pebble shale unit, Hue Shale, and Canning Fm.).	14
3	65-55									Deposit Tp (Paleocene part of Canning Fm.).	8
4	55-47									Deposit Tel (Mikkelsen Tongue of Canning Fm.).	8
5	47-37	7.5	1.5	6	15					Build and erode Sadlerochit and Shublik mountains anticlinoria.	7
6	37-34									Deposit Teu (Eocene part of Sagavanirktok Fm.).	5
7	34-32									Deposit To (Oligocene part of Sagavanirktok Fm.).	4
8	32-22					7.4	7.8			Northward propagation of basement duplex; creation & erosion of Marsh Creek anticline; renewed uplift and erosion of Sadlerochit and Shublik mtns. anticlinoria.	4
9	22-0							1	1.8	Deposit Tplm (Miocene to Pliocene part of Sagavanirktok Fm.); breakthrough at Shublik and Sadlerochit mtn. Fronts.	*

* No thermal calculations were made for this state.